2014

Expression and Splicing of Alzheimer's Disease Risk Gene Phosphatidylinositol-Binding Clathrin Assembly Protein

Ishita Parikh
University of Kentucky, lparikh19@gmail.com

STUDENT AGREEMENT:

I represent that my thesis or dissertation and abstract are my original work. Proper attribution has been given to all outside sources. I understand that I am solely responsible for obtaining any needed copyright permissions. I have obtained needed written permission statement(s) from the owner(s) of each third-party copyrighted matter to be included in my work, allowing electronic distribution (if such use is not permitted by the fair use doctrine) which will be submitted to UKnowledge as Additional File.

I hereby grant to The University of Kentucky and its agents the irrevocable, non-exclusive, and royalty-free license to archive and make accessible my work in whole or in part in all forms of media, now or hereafter known. I agree that the document mentioned above may be made available immediately for worldwide access unless an embargo applies.

I retain all other ownership rights to the copyright of my work. I also retain the right to use in future works (such as articles or books) all or part of my work. I understand that I am free to register the copyright to my work.

REVIEW, APPROVAL AND ACCEPTANCE

The document mentioned above has been reviewed and accepted by the student's advisor, on behalf of the advisory committee, and by the Director of Graduate Studies (DGS), on behalf of the program; we verify that this is the final, approved version of the student's thesis including all changes required by the advisory committee. The undersigned agree to abide by the statements above.

Ishita Parikh, Student

Dr. Steven Estus, Major Professor

Dr. Bret Smith, Director of Graduate Studies

Expression and Splicing of Alzheimer's Disease Risk Gene Phosphatidylinositol-Binding Clathrin Assembly Protein

---

DISSERTATION

A dissertation submitted in partial fulfillment of the
requirements for the degree of Doctor of Philosophy in the
College of Medicine
at the University of Kentucky

By

Ishita Jatin Parikh

Lexington, Kentucky

Director: Dr. Steven Estus, Professor of Physiology

Lexington, Kentucky

2014

ABSTRACT OF DISSERTATION

EXPRESSION AND SPLICING OF ALZHEIMER'S DISEASE RISK GENE PHOSPHATIDYLINOSITOL-BINDING CLATHRIN ASSEMBLY PROTEIN

Recent Genome Wide Association Studies (GWAS) have identified a series of single nucleotide polymorphism (SNP)s that are associated with Alzheimer's disease (AD). One of the SNPs, rs3851179 (G/A), is near the gene phosphatidylinositol-binding clathrin assembly protein (*PICALM*). To evaluate whether this SNP is associated with *PICALM* expression, we quantified *PICALM* mRNA in 56 brain cDNA samples. Using linear regression analysis, we analyzed *PICALM* expression relative to rs3851179, AD status, and cell type specific markers. An association was detected between rs3851179 and *PICALM*, microvessel mRNA, glial fibrillary acidic protein (GFAP) mRNA, and synaptophysin (SYN) mRNA. To gain clarity into other possible SNP mechanisms, we searched brain cDNA for *PICALM* splice variants. We identified several *PICALM* splice variants involving exons 13-19. To identify and gain an estimation of relative abundance of splice variants, we PCR-amplified across exons 13-20 in cDNA from six individuals, three rs3851179 GG individuals and three rs3851179 AA individuals. Sequencing the cloned isoforms we found that *PICALM* lacking exon 13 (delta 13) is the most abundant isoform. Other isoforms detected included deletion of exon 18-19. We targeted the latter part of the gene, exon 17-20, to investigate unequal allelic expression using next generation sequencing. Individuals heterozygous for rs76719109 (n= 35), located in exon 17, were used to study the abundance of G/T allele in cDNA and genomic DNA. When we analyzed the T:G allelic ratio, the variant lacking exons 18 and 19 showed unequal allelic expression (p-value < 0.001) in a subset of individuals. One individual was an outlier, showing overall unequal allelic expression, which maybe be harboring a rare mutation capable of modifying *PICALM* expression. The *PICALM* intronic SNP rs588076 was associated with delta 18-19 isoform splicing (p-value < 0.001). In conclusion, this study gained a greater insight into the role of AD genetics in PICALM expression and splicing.

KEYWORDS: PICALM, Alzheimer's disease, Next-generation sequencing, allelic expression imbalance, single nucleotide polymorphism

Ishita Jatin Parikh

October 16, 2014

EXPRESSION AND SPLICING OF ALZHEIMER'S DISEASE RISK GENE PHOSPHATIDYLINOSITOL-BINDING CLATHRIN ASSEMBLY PROTEIN

By

Ishita Jatin Parikh

Steven Estus, Ph.D.

Director of Dissertation

Dr. Bret Smith, Ph.D.

Director of Graduate Studies

October 16, 2014

Dedicated to my grandparents: Raman, Leela, Vastupal, and Vilas.

For your love, inspiration, blessings and so much more.

ACKNOWLEDGEMENTS

"Educating the mind without educating the heart is no education at all."

-Aristotle

When I embarked on this journey, I had hoped to gain knowledge and a path to a career. What I gained was training, expertise, experiences, mentorship, and friendships. It is enormously difficult to express my gratitude to all those who have made this a reality.

Firstly, I would like to thank University of Kentucky, College of Medicine-Physiology and Sanders Brown Center on Aging for giving me this opportunity. To Dr. Steven Estus, for the guidance and encouragement he has provided me over the years. I admire your intellect, professional scholarship, and generosity. I am grateful for your mentorship, which has empowered me grow both as a scientist and as a person. I would also like to thank my committee members: Dr. Donna Wilcock, Dr. Elizabeth Head, Dr. Stefan Stamm, Dr. Brian Delisle and Dr. David Fardo. It has truly been a pleasure having you on my committee. Thank you for your time, helpful advice and support.

For the past five years, the Estus lab has been a supportive environment, where I have not only engaged in critical thinking and scientific discussion, but have had profound conversations on philosophy, politics, and ethics. I especially want to thank James F Simpson for his patience, research acumen and wisdom. The conversations I have had with you have inspired me to be more self aware and mindful. I would also like to thank past lab members I-Fang Ling and Christopher Simmons, for welcoming me into the lab and assisting me during my first year in lab. To Manasi Malik, your brilliance is an inspiration. You have a bright future and I am grateful to be in your present.

I am grateful for the many wonderful people that have come into my life during my stay in Lexington. The friendships and bonds formed have made this journey special. To Kara Larson, you are like a superhero to me. Your

determination and honesty encourages me. I am so glad I made you give me a ride during orientation. I'm grateful that this PhD experience has brought us into each other's lives. To Sony Soman and Melissa Bradley-Whitman, thank you for making me come out of my third floor lab and making my PhD experience more enjoyable. Both of you are kind and caring and I am lucky to have met you. To Mansi Sethi, Aman Preet Dhillon, Subrahmanyam, Rahul Butala, and Anirban Chakraborty, thank you for your thoughtfulness and generosity. I cherish your friendship and only wish you had entered my life sooner. To my childhood friends Maria Lowe, Ashley Watkins and Casey Donavan, you are my constant. Thank you for always being a phone call away, for listening and caring. I cherish our friendship. I would like to thank Daxa and Dinesh Patel for making Lexington a home for me. I would also like to thank my family and relatives. I'm indebted to you for your well wishes, thoughts and prayers.

Lastly, this dissertation would not have been possible without the support of my family. To Ishan Parikh, I am thankful to you for always wishing the best for me and being proud of my achievements, even when I'm not. I am grateful that our parents procreated and produced you. Life would be boring without you in it. I'm indebted to Jatin and Lina Parikh, I am where I am because of you. Thank you for instilling in me the morals and values that help me succeed in life. You have always being there when I've needed you and I admire the scarifies that you have made at times to put my needs above yours. Thank you for raising me to be independent and strong. To papa, thank you for always giving me the courage and pushing me out the door to achieve bigger and better things. Thank you for having the confidence in me, even when I do not, and always encouraging me to make my own choices. To mummy, thank you for your love and friendship. Your intelligence, hard-work ethic and tenacity inspire me. I strive to achieve even a fraction of your fortitude and resilence. I hope to make you proud. Thank you again, for helping me and motivating me to achieve this.

TABLE OF CONTENTS

List of Tables

List of Figures

Chapter 1
Introduction

Alzheimer's Disease

Impact

Alzheimer's Disease (AD) is a complex disease with a genetic component that affects the aging population. An estimated 5.2 million people in the United States and 35.6 million worldwide are affected by the disease. Although dementia is seen in various neurodegenerative diseases, with an estimate that one in eight older Americans is diagnosed with dementia, AD is the most common cause of dementia. Prevalence of the disease will increase as the world's population ages and lives longer due to better healthcare and medical advances. Recent projections indicate that by 2030, when the baby boomers will be at least 65 years old, there will be more than a 50% increase from the current 5.2 million people affected. The burden of AD treatment cost can be felt both by healthcare programs, as well as the family and friends of the patient that provide care while forsaking their income and financial security for a challenging and stressful environment. The combined direct and indirect cost of AD is estimated to be $214 billion and the projected cost for 2050 balloons to 1.2 trillion dollars (Fargo & Bleiler, 2014).

History

In 1901, the first case of AD was identified in patient Auguste Deter by German psychiatrist Alois Alzheimer. Alzheimer followed the case until her death in 1906. Through Alzheimer's extensive notes we know that Auguste exhibited memory deficits, cognitive decline, and paranoia. The autopsy of Auguste's brain showed atrophy and arteriosclerosis of blood vessels (Maurer, Volk, & Gerbaldo, 1997). Alzheimer's observed, described and illustrated numerous neurofibrillary tangles and amyloid plaques. Thus patients with dementia and this neurohistological pathology have subsequently been diagnosed with a disease that bears his name, Alzheimer's Disease. Although AD is the most common cause of dementia, there are other types of dementia that can be present, such as vascular dementia or frontotemporal lobar degeneration. Thus an autopsy is the only definitive way to diagnose AD.

Diagnosis

Clinically, AD and other causes of dementia are diagnosed by neurological exam and mental status tests. One of the commonly used mental exams is the Mini-mental state exam (MMSE), where a patient answers a series of questions designed to test cognition. It tests the patient's ability to follow verbal and written commands, as well as memory, attention, and orientation. The total maximum score for the test is 30 (Folstein, Folstein, & McHugh, 1975). An MMSE score of less than 12 suggests severe dementia, whereas 13-20 is considered moderate and 20-24 is mild cognitive decline (Fargo & Bleiler, 2014).

Histopathologically, the brain is evaluated for neurofibrillary tangles and senile plaques to be diagnosed for AD. Braak Stage classifies extent of neurofibrillary tangle accumulation and distribution. There are a total of six Braak stages, and severity of diagnosis increases with each stage (Braak & Braak, 1991). The Consortium to Establish a Registry for Alzheimer's disease (CERAD)

score evaluates and ranks the density of neuritic plaques in the brain (Mirra et al., 1991). Lastly, NIA-Reagan Institute Criteria (NIARI) combines both the CERAD and Braak stage scores and evaluates patient's likelihood of AD neuropathologically (Hyman & Trojanowski, 1997).

Although amyloid plaques and neurofibrillary tangles are two hallmarks of AD, there are other lesser known lesions and proteins that are also seen in AD; such as Hirano bodies, TDP-43, Lewy bodies and granulovacuolar degeneration (Perl, 2010; Wilson, Dugger, Dickson, & Wang, 2011). Diagnosis of AD is varied and through clinical and histopathological criteria, clinicians and researchers aim to have a more concise conclusion of diagnosis. Apart from the neurological exams, clinicians have limited tools to diagnose AD. Currently, there are no biomarkers or imaging tools to diagnose AD. Cerebrospinal fluid (CSF) $A\beta_{40}$ and $A\beta_{42}$ levels are being examined by researchers and clinicians as a tool to diagnose AD and assess the progression of mild cognitive impairment to AD. Having a more sensitive assessment of AD outcome could lead to early detection and a better therapeutic profile (Shaw et al., 2009). Decreased levels of $A\beta_{42}$ in CSF have been seen as a biomarker of AD-related pathologic changes in the brain; suggesting more accumulation of $A\beta$ in the brain and less clearance (Blennow & Hampel, 2003). Neuroimaging is also another venue for AD diagnosis. Pittsburgh compound B (PiB) is a radioactive compound that binds to amyloid plaque. PiB has shown promising results in imaging amyloid deposits in brain scans in patients (Klunk et al., 2004). The amount of amyloid plaque load in a brain scan, in combination with $A\beta_{1\text{-}42}$ in CSF could pave way to helping diagnose patients at an earlier stage of AD.

Etiology

Neuritic or senile plaques consist of amyloid beta peptide ($A\beta$) aggregate deposits in the extracellular matrix of brain. $A\beta$ peptide is a fragment of the Amyloid Precursor Protein (APP) (Glenner & Wong, 1984; Kang et al., 1987).

Located on the long arm of chromosome 21, *APP* is a highly conserved gene presenting multiple isoforms. Although APP is ubiquitously expressed, it is highly expressed in brain and kidney. In brain, APP function is still unclear. It has been implicated in neuronal development, survival and synaptic density (Oh et al., 2009; Roch et al., 1994; Young-Pearse et al., 2007).

APP processing is critical in developing AD (**Figure 1.1**). APP can be proteolyzed by α, β, and γ-secretase to produce multiple products, including Aβ. When APP is cleaved by β-secretase and subsequently γ-secretase, proteolysis generates Aβ peptide that is 39-42 amino acids. $A\beta_{42}$ is the more toxic species of these peptides; they aggregate and form plaques in the extracellular space. Although $A\beta_{42}$ only accounts for 10% of the Aβ peptide product, it is associated with AD plaque pathology; because of its hydrophobic nature it is more inclined to fibril formation, and resist proteolytic degradation and clearance (Burdick et al., 1992; Selkoe, 1998). High Aβ load has been shown to disrupt synaptic function and cause neuronal death (Deshpande, Mina, Glabe, & Busciglio, 2006; Shankar & Walsh, 2009). A tremendous amount of research has been done on the amyloid cascade pathway, however the role environmental and genetic factors play in APP processing and Aβ aggregation in propagating sporadic AD is still unclear.

Neurofibrillary tangles, another hallmark of AD, consists of hyperphosphorylated tau protein within the neuronal cytoplasm. Tau is a microtubule binding protein found mostly in neuronal cells axons and functions to stabilize microtubules. Alternate splicing of microtubule-associated protein tau (MAPT) gene, located on chromosome 17, produces multiple isoforms with variable microtubule-binding and phosphorylation sites (Hanger et al., 2007). When attached to the microtubules, tau allows the microtubules to be structured tracks for axonal transport of vesicles. Typically, tau detaches from the microtubules temporarily when phosphorylated, allowing for flexibility. When tau protein is hyperphosphorylated, it destabilizes and detaches from the

microtubules, causing tau aggregates to form within the neuron (Grundke-Iqbal et al., 1986; Schneider, Biernat, von Bergen, Mandelkow, & Mandelkow, 1999). Tau tangles have also, like Aβ, been associated with neuronal death and synaptic dysfunction (Gamblin et al., 2003; Tai et al., 2012). AD brains have more abundant and different phosphorylation sites; current therapeutic targets focus on modulating tau phosphorylation through specific kinase inhibitors (Hanger et al., 2007; Mudher et al., 2004; Noble, Hanger, Miller, & Lovestone, 2013).

Susceptibility

There are two forms of AD: early onset AD and late onset AD. Early onset AD or familial AD (FAD) is a rare form of AD and is characterized by being affected by dementia at a young age (younger than 65 years old). FAD can have Mendelian autosomal dominant form of heredity and can be passed on through generations. Through genetic linkage analysis studies gene mutations responsible for FAD were discovered. A missense mutation near the β-secretase cleavage in APP was the first mutation associated with FAD (Goate et al., 1991). Mutations in primarily three genes have been linked to FAD: APP, Presenilin-1 (PSEN1), and Presenilin-2 (PSEN2) (Schellenberg et al., 1992; Sherrington et al., 1995). Since the early 90s, many mutations have been linked with FAD, involving APP processing and Aβ production, particularly near enzymatic cleavage sites. Currently, there are 238 mutations residing in these three genes that have been studied for AD. PSEN1 exhibits 185 mutations with pathogenic effect and is represented highest in familial genetic screening (Cruts, Theuns, & Van Broeckhoven, 2012). There are other genes with mutations that have been linked to FAD to a lesser extent, such as FUS, GRN, MAPT, TARDBP, VCP and C9orf72. PSEN1 and PSEN2, located on chromosome 14 and 1, respectively, are part of γ-secreatase complex that cleaves APP to subsequently produce Aβ. Mutations within these genes have been shown to increase Aβ40/Aβ42 ratio (Steiner, 2004). Mutations in MAPT have also been linked to FAD, thus piquing

researchers' interest in studying genotype influencing the development of pathogenic phenotype, specially in Late On-set AD (LOAD) (Cruts et al., 2012).

LOAD is the sporadic form of AD with age of onset being 65 or older. LOAD accounts for up to 95% of AD cases (Eisenstein, 2011). Twin studies suggest that approximately 79% of AD is genetic (Avramopoulos, 2009; Gatz et al., 2006). A primary genetic risk factor for AD is apolipoprotein E (APOE). Three most common variants of APOE include E2, E3, and E4; one copy of E4 increases AD risk by 4 fold and two copies by 12-fold (Eisenstein, 2011; O'Brien & Wong, 2011). APOE gene is found on chromosome 19 and encodes for a protein that facilitates the transport of lipoproteins throughout the body.

APOE is primarily produced by microglia and astrocytes in the brain. There are several proposed mechanisms through which APOE can modulate AD pathology. The primary result shows Aβ clearance is influenced in APOE allele dependent manner, where Aβ clearance is disrupted by E4 the most. Aβ binds lipidated APOE and is cleared through the blood brain barrier (Liu, Kanekiyo, Xu, & Bu, 2013)

Beyond APOE, researchers have struggled to find single nucleotide polymorphism (SNP)s that influence AD onset. It has been difficult to identify genes or genetic factors that modulate the disease. Although these variants alone are variable in the whole disease population, however the combination of different sporadic SNPs may be carried by AD population that affect a gene or genes in the same pathway and consequently influence disease onset and progression. Due to the heterogeneity of AD, it has been difficult to find risk genes with small cohorts and with enough statistical significance.

Genetics of AD

Genome-wide association studies (GWAS) have revolutionized the search for low penetrative alleles that influence risk for complex diseases and traits. Associations made between the genetic variations and phenotype are within a

large sample size and span the whole genome, enabling researchers to discover risky or protective loci. Over the last couple of years, GWAS have identified many risk loci and candidate genes for AD by genotyping SNPs in AD and non-AD groups. (Bertram, McQueen, Mullin, Blacker, & Tanzi, 2007). APOE remains the highest risk factor for AD within GWA studies, but loci around *BIN1*, *CLU, ABCA7, CR1, PICALM, MS4A6A, CD33, MS4A4E*, and *CD2AP* have been implicated in AD and are currently the top ten risk genes on Alzgene (Bertram et al., 2007). As more studies are conducted in different cohorts and populations, additional loci have been implicated in AD, including *EPHA1, INPP5D, MEF2C, HLA-DRB1-HLA-DRB5, NME8, SLC24A4/RIN3, ZCWPW1, PTK2B, SORL1, CELF1, FERMT2, DSG2* and *CASS4* (Lambert et al., 2013).

Understanding how these SNPs are associated with AD is complex for several reasons. First, the association of these SNPs with AD risk does not indicate causality of AD phenotype or pathology. Rather, these SNPs contribute to risk and have low penetrance. Second, discerning the gene associated with the AD-associated SNP is challenging if multiple genes are present within the same genetic linkage disequilibrium (LD) block as the implicated SNP. Third, a large number of these SNPs are not genotyped but imputed based on their LD with a genotyped SNP. Thus there is ambiguity about the functional SNPs and genes associated with AD. As more GWA studies and meta-analysis studies are conducted there is more confidence within loci. Lastly, the effect of these SNPs on AD risk is small such that the accumulated risk of these SNPs may be more relevant. Considering that many of the SNPs implicate genes within similar pathways, such as cholesterol homeostasis, inflammation and endocytosis, some interaction among the SNPs within a pathway may become clear with further studies. Of particular relevance here, several SNPs in genes associated with endocytosis have been associated with AD, including SNPs within *BIN1, CD2AP,* and *PICALM*.

PICALM is associated with LOAD through multiple GWAS studies. *PICALM* is located on chromosome 11 with the primary SNP, rs3851179, ~80,000bp 5' upstream of *PICALM.* The minor allele of this SNP reduces AD risk with an odds ratio ~0.88. Several other *PICALM* SNPs have also been associated with AD risk: rs561655, rs592297 and rs541458 (Corneveaux et al., 2010; Harold et al., 2009; Hollingworth et al., 2011; Jun et al., 2010; Lambert et al., 2013; Naj et al., 2011; Schjeide et al., 2011). The initial studies were primarily performed with Caucasian populations, however when studies were replicated and/or performed with different populations, there was no association found between AD risk and SNP in Italian, Hispanic, and Chinese populations (Lee et al., 2011; Piaceri et al., 2011; Yu et al., 2011). This difference can be interpreted as either (i) the SNP effect may be population specific or (ii) these conflicting results maybe due to small sample size of the studies, as positive associations were seen in other studies and meta-analysis (Feinkohl et al., 2013; T. Jiang et al., 2014; G. Liu et al., 2013; Miyashita et al., 2013)

Clathrin Mediated Endocytosis and PICALM

PICALM functions to assist in clathrin coated pit formation. Normal regulation of Clathrin Mediated Endocytosis (CME) is critical for cellular homeostasis. CME is essential for cellular functions such as cell-to-cell communication, cell surface protein regulation and protein recycling. Different proteins facilitate clathrin coat formation through distinct stages of coat development (Ramanan et al., 2011b). These proteins, including PICALM, are collectively called clathrin assembly proteins. PICALM binds phosphatidylinositol 4,5-bisphosphate (PIP_2), adaptor protein 2 (AP_2), and clathrin. PIP_2 is abundantly present in plasma membrane. Clathrin and AP_2 are involved in the early phase of vesicle formation, which consists of nucleation and invagination. PICALM contains a N-terminal globular PIP_2 binding module called ANTH (AP180 N-terminal Homology) domain (Dreyling et al., 1996). PICALM motifs that bind AP_2

include ^{375}DIF, ^{420}DPF and ^{489}FESVF, which are encoded by exons 11, 13, and 14, respectively. PICALM motifs that bind clathrin are primarily in the PICALM C-terminal region and secondarily a weak binding site at the ^{392}DLLDLQ motif encoded by exon 12 (Dreyling et al., 1996; Meyerholz et al., 2005) (**Figure 1.2**). Organization of the clathrin coat is influenced by PICALM as the size and shape of clathrin-coated vesicles is altered with overexpression or knockdown of PICALM (Meyerholz et al., 2005; Tebar, Bohlander, & Sorkin, 1999).

PICALM and AD

APP trafficking and cleavage appears central to development of AD. CME plays a role in APP internalized from the cell membrane and subsequent amyloid beta generation, suggesting a possible relationship PICALM could have with AD. CME proteins, including PICALM, are significantly increased in transgenic mice AD (Koo & Squazzo, 1994; Thomas, Lelos, Good, & Kidd, 2011). In neurons, PICALM has been shown to influence cell surface protein endocytosis and recycling (Harel, Mattson, & Yao, 2011). The function of PICALM in AD is perplexing. There are conflicting results on how PICALM could modulate AD pathology. In yeast, mice and rat models, increased PICALM has been shown to increase Aβ production (Treusch et al., 2011; Xiao et al., 2012). However, *in vitro* show that increased PICALM results in decreased endocytosis of transferrin (Tebar et al., 1999). It has been proposed that PICALM may function in a cargo specific manner.

Significance of the Study

Recent advances in GWAS have provided insights into AD genetics. GWAS scans though the human genome for SNPs which associate with disease. Recent studies with large populations identified several risk genes for AD, including *PICALM*. Though these SNPs may have a modest effect, they have been replicated with significance numerous times in different populations. Although GWAS can identify genetic variant associations, there is a lack of functional link between the genetic variants and AD. This study aims to

characterize the link between *PICALM* genetic association with AD. *PICALM* is part of the clathrin assembly protein family and the encoded protein assists in clathrin coat formation in clathrin-mediated endocytosis. PICALM assists clathrin coat formation by scaffolding AP_2 and clathrin to generate a clathrin coated pit. Genetic variant rs3851179, located upstream of *PICALM*, was associated with AD. In this study we hypothesize that rs3851179 is associated with *PICALM* expression or splicing.

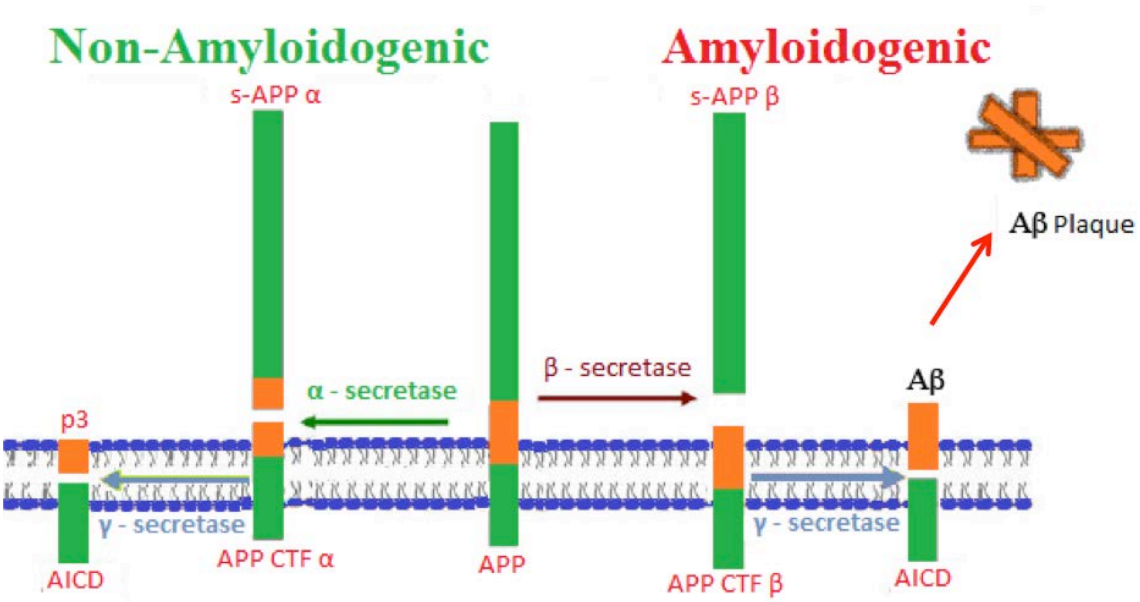

Figure 1.1 APP Processing.

In the non- amyloidogenic pathway, APP is proteolytically cleaved by α secretase and subsequently by γ secretase to produce soluble APP (s-APP α and p3, respectively. In the amyloidogenic pathway, APP is cleaved by β secretase and γ secretase resulting in s-APP β and Aβ fragment, respectively. Accumulation of Aβ fragments results in amyloidogenic plaque.

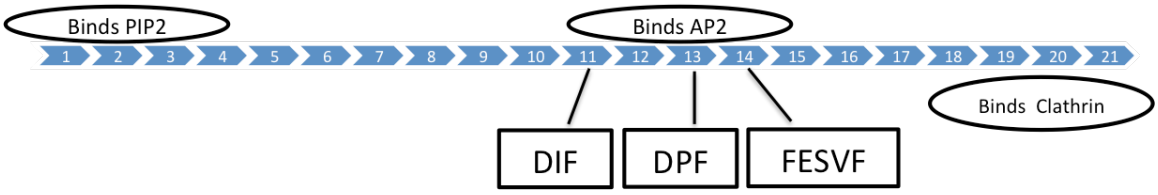

Figure 1.2 PICALM Exons, Protein Binding Sites and Critical Protein Motifs

PICALM encodes protein motifs and domains important for binding to PIP_2, AP_2 and clathrin. This gene schematic shows the 21 PICALM exons. N-terminus of PICALM binds PIP_2 via the ANTH domain. ANTH domain is encode by several exons, diagram not to scale. Three motifs important for effective PICALM binding to AP_2 is encoded by exons 11, 13, and 14 and c-terminus of PICALM binds to clathrin (Meyerholz et al., 2005).

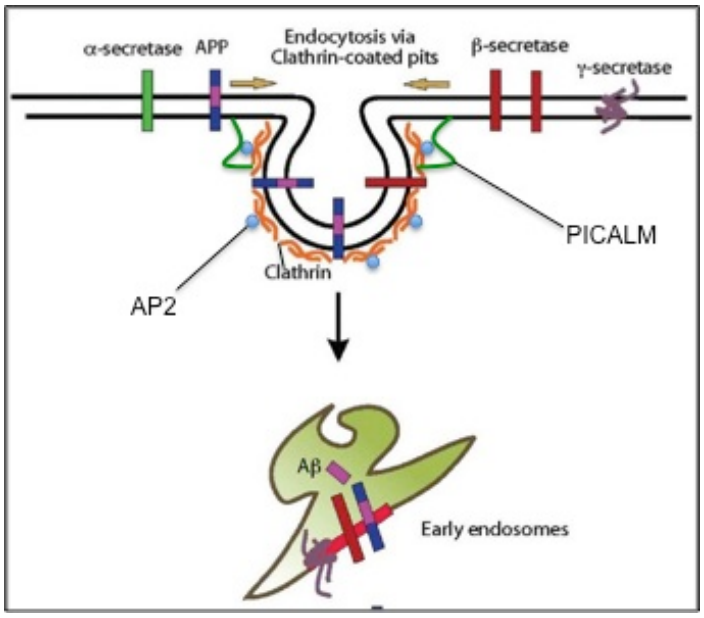

Figure 1.3 PICALM Pathogenic model

Clathrin and cargo molecules are assembled into clathrin-coated pits on the plasma membrane together with an adaptor protein 2 (AP_2) that links clathrin with transmembrane receptors, concluding in the formation of mature clathrin-coated vesicles (CCVs). CCVs are then actively uncoated and transported to early/sorting endosomes. PICALM binds to PIP_2 on the plasma membrane, while also binding with AP_2 and clathrin.

Adapted from: (Bali et al., 2010)

Chapter 2
Genetics of *PICALM* Expression and Alzheimer's Disease

Abstract

Novel Alzheimer's disease (AD) risk factors have been identified by genome-wide association studies. Elucidating the mechanism underlying these factors is critical to the validation process and, by identifying rate-limiting steps in AD risk, may yield novel therapeutic targets. Here, we evaluated the association between the AD-associated polymorphism rs3851179 near *PICALM*, which encodes a clathrin-coated pit accessory protein. Immunostaining established that PICALM is expressed predominately in microvessels in human brain. Consistent with this finding, *PICALM* mRNA expression correlated with expression of the endothelial genes *vWF* and *CD31*. Additionally, we found that PICALM expression was modestly increased with the rs3851179A AD-protective allele. Analysis of *PICALM* isoforms found several isoforms lacking exons encoding elements previously identified as critical to PICALM function. Increased expression of the common isoform lacking exon 13 was also associated with the rs3851179A protective allele; this association was not apparent when this isoform was compared with total *PICALM* expression, indicating that the SNP is associated with total *PICALM* expression and not this isoform per se. Interestingly, *PICALM* lacking exons 2-4 was not associated with rs3851179 but was associated with rs592297, which is located in exon 5. Thus, our primary findings are that multiple *PICALM* isoforms are expressed in the human brain, that PICALM is robustly expressed in microvessels, and that expression of total *PICALM* is modestly correlated with the AD-associated SNP rs3851179. We interpret these results as suggesting that increased *PICALM* expression in the microvasculature may reduce AD risk.

Introduction

Alzheimer's disease (AD) is a devastating disease marked by cognition and memory decline, affecting the elderly population. Twin and family-based studies suggest that sporadic late onset AD risk is genetically linked (Avramopoulos, 2009; Gatz et al., 2006). Recent genome wide association studies (GWAS) have identified loci of genetic variance, single nucleotide polymorphisms (SNP)s, that are associated with AD risk (Harold et al., 2009; Hollingworth et al., 2011; Jun et al., 2010; Lambert et al., 2009; Lambert et al., 2011; Naj et al., 2011). Elucidating the mechanism of action of these SNPs validates the SNP as an AD risk factor and may identify novel AD pathways. Additionally, since steps in AD pathways that are modulated by genetics may be susceptible to pharmacologic manipulation, identifying the actions of AD-associated SNPs may lead to robust new pharmacologic targets.

One of these SNPs is near the gene *PICALM* (phosphatidylinositol binding clathrin assembly protein) which is involved in endocytosis. The primary AD-associated SNP is rs3851179, which lies approximately 80 kb 5' of *PICALM*(Hollingworth et al., 2011; Morgan, 2011; Naj et al., 2011). *PICALM* itself is encoded by 21 exons, several of which are variably spliced (Flicek et al., 2014). Here, we sought to elucidate how rs3851179 alters *PICALM* expression or splicing to modulate AD risk. We report that PICALM is expressed robustly in microvessels and moderately in other cell types. Rs3851179 was modestly associated with total *PICALM* expression as well as the major *PICALM* isoform lacking exon 13. In contrast, the expression of rare *PICALM* isoforms lacking exons 2, 2-4, or 18-19 was not associated with rs3851179. We interpret our results as suggesting that the PICALM is robustly expressed in microvessels and that the protective rs3851179A allele is associated with modestly increased *PICALM* expression. We speculate that increased microvessel *PICALM* reduces AD risk, perhaps by facilitating Aβ clearance from the brain through enhanced translocation across the blood brain barrier.

Materials and Methods

Ethics Statement

The work described here was performed with approval from the University of Kentucky Institutional Review Board.

Tissue samples

The RNA and DNA samples for this study were from de-identified AD and non-AD autopsy samples. Anterior cingulate specimens were provided by the University of Kentucky AD Center Neuropathology Core and have been described previously (Ling, Bhongsatiern, Simpson, Fardo, & Estus, 2012; Malik et al., 2013). A total of 52 brain samples, 28 male and 24 female, were used for this study. All of the non-AD individuals were cognitively intact at their last visit (MMSE of 27.9 ± 3.4 (mean ± SD)). AD individuals were demented (MMSE of 12.2± 8.3). For the AD autopsy samples, the average age at death and postmortem interval was 82.9 ± 6.4 years (mean ± SD) and 3.4 ± 0.7 hrs, respectively. For the non-AD samples, the average age at death and postmortem interval was 82.3 ± 8.7 years (mean ± SD) and 2.8 ± 0.8 hrs, respectively. By NIARI neuropathology criteria, the non-AD individuals included 21 samples with a score of no-low likelihood of AD, and 6 with intermediate. The AD samples were uniformly high-likelihood of AD. RNA was prepared by the method of Chomczynski and Sacchi (Chomczynski & Sacchi, 1987) and converted to cDNA with random hexamers and Superscript II, as described previously (Ling et al., 2012). Although RNA integrity analyses were not performed prior to reverse transcription, others have demonstrated that for qPCR with short amplicons, normalized expression differences are comparable between samples with moderate RNA degradation and those with high integrity RNA (Fleige & Pfaffl, 2006).

PICALM immunostaining

Paraffin-embedded anterior cingulate tissue sections (5 µm thick) were rehydrated, underwent heat-induced antigen retrieval in citrate buffer (pH 6.0) and were quenched in 0.3% H_2O_2. Sections were immersed in 10% rabbit serum in Tris-buffered saline followed by an overnight incubation in anti-CALM (sc-6433, Santa-Cruz; 1:400 dilution). After thorough rinsing in Tris-buffered saline, sections were incubated in biotinylated secondary antibody for 1 h, rinsed, incubated in ABC reagent (Vector) for 1 h, developed in Nova Red chromagen (Vector) and counterstained with Hematoxylin.

Identification of PICALM Splice Variants in Human Brain

Screening for *PICALM* splice variants was performed on a pool of cDNA samples from five AD and five non-AD individuals. This cDNA pool was amplified by PCR by using forward and reverse primers designed to produce overlapping products; this enabled evaluation of splicing efficiency of each internal exon (Table 2.1). The identity of splice variants was determined by sequencing. To estimate the distribution of these splice variants, exon 12-20 PCR products from three rs3851179 homozygous minor (A/A) and three homozygous major (G/G) individuals were TA-cloned (Invitrogen) and 847 random clones were sequenced. For this work, thirty cycles of PCR (Platinum Taq, Invitrogen) were performed by using primers corresponding to exons 12 and 20 (Table 2.1). PCR conditions were 94° for 15 seconds, 60° for 15 seconds, and 72° for 60 seconds (Veriti 96-Well Thermal Cycler, Life Tech). PCR was conducted using approximately 30 ng of cDNA template. After PCR, samples were cloned into pcDNA2.1 according to the manufacturer's instructions (TA-Cloning Kit, Invitrogen) and sequenced.

Quantitation of PICALM Expression

Total *PICALM* expression was quantified by qPCR using primers corresponding to sequences within the constitutively present exons 9 and 10 (Table 2.1); *PICALM* isoforms lacking exon 2, exons 2-4, 13 or 18-19 were quantified similarly (Table 2.1). As no single Ensembl transcript incorporates

each of the exons that we identify here, note that our exon designations are derived from ENST00000393346 for exons 1-16. Exons 17-21 correspond to the final five exons within ENST00000532317. PCR was conducted using an initial 2-minute incubation at 95°, followed by cycles of 10 seconds at 95°, 20 seconds at 60°, and 20 seconds at 72°. The 20 μL reactions contained 1μM of each primer, 1x PerfeCTa SYBR Green Super Mix (Quanta Biosciences), and 30 ng cDNA. Experimental samples were amplified in parallel with serially diluted standards that were generated by PCR of cDNA using the indicated primers followed by purification and quantitation by UV absorbance. Results from samples were compared relative to the standard curve to calculate copy number in each sample. Real time assays were performed at least twice and the average copy number used for data analyses. Since *PICALM* was expressed in microvessels, neurons and astrocytes, we wished to compare *PICALM* expression to that of genes specific to these cell types. Hence, we also quantified two microvessel-specific mRNAs, *CD31* and von Willebrand Factor (*vWF)*, neuron-specific mRNA *SYP* and astrocyte-specific *GFAP.* (Jackson, 2003; Sadler, 1998). The copy number for each mRNA was then normalized to the geometric mean of reference genes *RPL32* and *EIF4H*, previously quantified in this sample set (Ling et al., 2012; Malik et al., 2013). The linear regression statistical model used to analyze the data included the geometric mean of *CD31* and *vWF* (microvessel mRNA), *GFAP, SYP,* AD status and the number of rs3851179 minor alleles (SPSS version 21).

Results

To begin to evaluate the role of *PICALM* in AD, we localized PICALM expression in human brain by performing immunohistochemistry. We used an antibody that recognizes an epitope at the extreme PICALM carboxyl terminus that is found in all *PICALM* isoforms (see below). Robust PICALM expression was observed in microvessels in both non-AD and AD brain sections (**Figure 2.1**). Consistent with other reports, we also observed less robust PICALM

immunostaining in other cell types that have been identified as neurons and glia (Ando et al., 2013; Baig et al., 2010).

To elucidate the impact of the primary AD-associated SNP rs3851179 on *PICALM*, we chose a three-tiered approach. First, we evaluated whether a non-synonymous *PICALM* SNP was in linkage disequilibrium with rs3851179. The rs3851179 minor allele frequency in European Americans is 35%. According to the Exome Variant Server (http://evs.gs.washington.edu/EVS/), there are no non-synonymous *PICALM* SNPs with a minor allele frequency above 0.2% ("Exome Variant Server,"). Hence, the rs3851179 association with AD is not likely to be explained by a non-synonymous *PICALM* SNP.

The second tier of our approach to elucidate SNP action was to evaluate the extent that *PICALM* expression correlated with rs3851179 genotype and/or AD status. To this end, total *PICALM* expression was quantified in 52 brain samples by using qPCR and primers corresponding to sequences within exons 9 and 10 which are constitutively present (see below). *PICALM* copy number was normalized to the geometric mean of two housekeeping genes, *RPL32* and *eIF4H* (Ling et al., 2012; Malik et al., 2013). Inspection of the results supports that total *PICALM* expression correlated positively with microvessel mRNA expression (**Figure 2.2A**). To evaluate the statistical correlation between *PICALM* expression and relevant indices, we analyzed *PICALM* expression relative to AD status, rs3851179 genotype, and several cell-type specific mRNAs. Linear regression analysis found an overall significant model (adjusted R^2=0.46) with a significant correlation between *PICALM* and rs3851179 as well as cell type markers but not AD (Table 2.2). Rs3851179, *GFAP* and microvessel mRNA correlated positively with total *PICALM* expression, whereas *SYP* showed negative correlation. The AD-protective, minor rs3851179A allele was associated with increased total *PICALM* expression.

The third tier of our approach to determine possible SNP function was to evaluate the extent that a *PICALM* splice variant was associated with rs3851179 genotype and/ or AD status. We began by identifying *PICALM* splice variants present in human brain. PCR was performed by using a series of primer pairs that flank *PICALM* internal exons, e.g., primers corresponding to exons 1 and 5 were used to evaluate whether exons 2, 3 or 4 were variably spliced. This study found that multiple *PICALM* exons were inefficiently spliced (**Figure 2.3**). Sequencing of the exon 1-5 amplicons found that most *PICALM* isoforms contained exons 2, 3 and 4 while apparently rare isoforms lacked exon 2 or exons 2- 4. Amplifying from exon 3 to exon 9, and exon 7 to exon 12 showed that exons 5-11 were consistently present (**Figure 2.3**). This supports the use of primers corresponding to exons 9 and 10 for qPCR for total *PICALM*. Amplification reactions between exons 10-21 overall found multiple *PICALM* isoforms. These isoforms were not sufficiently resolved by polyacrylamide gel electrophoresis to allow sequencing of individual gel-purified products. To overcome this issue, *PICALM* from exon 12 to exon 20 was PCR-amplified, and the PCR products cloned and sequenced. To gain an initial evaluation of whether rs3851179 may be associated with *PICALM* splice variants, we analyzed RNA from three rs3851179 G/G and three rs3851179 A/A homozygous individuals. This effort revealed that exons 13, 14, 18 and 19 were inefficiently spliced. The most common *PICALM* variant lacked exon 13 and contained each of the other exons from 12 to 20 (Table 2.3). Other common variants contained each exon from 12-20, or lacked exon 13 and the initial 15 bp of exon 15, or lacked both exon 13 and 18. A comparison of the abundance of each isoform in rs3851179G/G versus rs3851179A/A individuals did not reveal striking differences (Table 2.3). Overall, we interpret these data as indicating that multiple *PICALM* exons are variably spliced. Although these isoforms were not associated with rs3851179 in this semi-quantitative assay, their abundance warranted a more quantitative evaluation.

For quantitation, we initially focused on exon 13 because (i) this exon is commonly skipped and (ii) this exon encodes the DPF peptide motif that contributes to PICALM binding to AP_2 (Meyerholz et al., 2005). We quantified *PICALM* lacking exon 13 (*D13-PICALM*) by using qPCR primers corresponding to sequences within exon 11 and the exon 12- exon 14 junction (Table 2.1). *D13-PICALM* correlated well with total *PICALM* expression and constituted about 40% of total transcript (**Figure 2.2B**). *D13-PICALM* expression was analyzed as a function of rs3851179, AD status, and several cell-type specific mRNAs. The expression of *D13-PICALM* correlated with rs3851179, AD status, as well as the cell-type specific mRNAs (adjusted R^2 =0.54, Table 2.2). The minor rs38555179A allele and the absence of AD correlated with increased *D13-PICALM* expression.

To evaluate whether rs3851179 was associated with *D13-PICALM* independently of the SNP association with total *PICALM* expression, we analyzed *D13-PICALM* expression as a function of rs3851179, AD status and total *PICALM* expression. With this analysis, we found that *D13-PICALM* was associated with AD status and total *PICALM*, but not rs3851179. Hence, *D13-PICALM* expression is associated with rs3851179 only because total *PICALM* expression is associated with rs3851179.

We next analyzed *PICALM* splice variants that lacked exons 18 and 19 (*D18-19 PICALM*), noting that the PICALM carboxyl region that includes amino acids encoded by exon 18 and 19 is critical for PICALM function (Scotland et al., 2012). This qPCR assay used forward and reverse primers that recognized exon 17 and the exon 17 - exon 20 junction, respectively (Table 2.1). We found that *D18-19 PICALM* represented 1-2% of total *PICALM* expression (**Figure 2.2C**) and correlated with neuronal and astrocyte content but not rs3851179 (Table 2.2).

We next quantified isoforms that lack exon 2 (*D2-PICALM*). This isoform is expected to not encode a functional protein because the loss of exon 2 introduces a codon frameshift with a premature stop codon in exon 3. Exon 2 encodes a portion of the ANTH domain that binds PIP_2 on the plasma membrane during the initial stage of clathrin-coated pit formation (Dreyling et al., 1996), We found that *D2-PICALM* was typically rare, representing less than 1% of total *PICALM* expression (**Figure 2.2D**). However, two samples showed increased *D2-PICALM* expression, ranging as high as 3.6%. The reason underlying the higher *D2-PICALM* in these individuals was unclear; these individuals both had AD, they differ in sex (one female and one male), and had a post-mortem interval similar to the other samples (2.4-4.0 hours). When these outlier samples were excluded from analysis, *D2-PICALM* was significantly associated with microvessel and neuronal content, as well as AD status but not rs3851179 genotype (adjusted R^2=0.41, Table 2.2). *D2-PICALM* was increased in AD individuals.

We also identified a *PICALM* isoform lacking exons 2-4 (*D2-4 PICALM*). The *D2-4 PICALM* isoform was also present at low levels, with an average of 0.28 ± 0.15% (mean ± S.E.) of total *PICALM* expression (**Figure 2.2E**). Expression of *D2-4 PICALM* was associated with AD but not with rs3851179 or microvessel content, suggesting that this variant is not expressed in microvessels (Table 2.2). Interestingly, Schnetz-Boutaud et al have reported that an exon 5 SNP rs592297 is in linkage disequilibrium with rs3851179 (D'=1, r^2=0.34) and proposed that rs592297 modulates the activity of an exon splicing enhancer (Schnetz-Boutaud et al., 2012). Therefore we evaluated whether rs592297 was associated with *D2-4 PICALM* expression. We found that rs592297 associated with the *D2-4 PICALM* (**Figure 2.2F**, Table 2.2). Hence, higher *D2-4 PICALM* expression is associated with the rs592297C minor allele. The percentage of *PICALM* expressed as *D2-4 PICALM* was quite low but was increased from 0.23 ± 0.11% in rs592297 major allele homozygous samples to 0.36 ± 0.17% in samples with the rs592297 minor allele (**Figure 2.2F**, p=0.004). Although we and

others have not examined the association of this SNP with AD directly, based on the linkage between rs592297 and rs3851179, the minor rs592297C allele is likely to associated with increased AD risk (Schnetz-Boutaud et al., 2012).

Discussion

The primary findings of this paper are (i) multiple *PICALM* isoforms are expressed in human brain, (ii) consistent with immunohistochemistry results that PICALM is commonly found in microvessels, expression of total *PICALM* and the abundant *D13-PICALM* is positively correlated with the expression of microvessel mRNAs, (iii) total *PICALM* expression correlates modestly with the AD-associated SNP rs3851179, (iv) *D2-4 PICALM* was associated with AD status and an exon five SNP, rs592297, which is in linkage disequilibrium with rs3851179 (r^2=0.34). However, *D2-4 PICALM* was a rare isoform, suggesting that this association is not responsible for the SNP association with AD, and (v) two additional rare *PICALM* isoforms, *D18-19 PICALM* and *D2-PICALM* were variably associated with AD and cell-specific mRNAs. Overall, we interpret our results as suggesting that multiple PICALM isoforms are expressed in the brain, and that correcting for cell-specific mRNAs allows the discernment that the AD-protective allele of rs3851179 is associated with increased *PICALM* expression.

Immunostaining showed abundant PICALM expression in microvessels. Consistent with this observation, total *PICALM* expression correlated with *CD31* and *vWF* expression, genes highly expressed in endothelial cells (Jackson, 2003; Sadler, 1998). Hence, our statistical model for *PICALM* expression included the geometric mean of these microvessel mRNAs, well as *SYP* and *GFAP*. When we analyzed *PICALM* expression in this fashion, *PICALM* expression correlated with rs3851179 genotype. Indeed, inclusion of the expression of these cell-type specific mRNA is the primary difference between our study which detected an association between PICALM expression and rs3851179 and prior studies that did not discern this association (Allen et al., 2012; Karch et al., 2012). The modest association that we observed may reflect that rs3851179 is not a

functional SNP but rather is in linkage disequilibrium with SNP(s) that directly modulate *PICALM* expression. Rs3851179 is unlikely to be a directly functional SNP since its well removed from *PICALM* at 80kbp upstream and does not alter a transcription factor binding site as predicted by ENCODE (Rosenbloom KR, 2012). Hence, we speculate that another SNP, more proximal to *PICALM*, is the functional SNP and is in moderate linkage disequilibrium with rs3851179.

Variation in *PICALM* expression associated with rs3851179 genotype may have several effects. At the cellular level, PICALM mediates clathrin-coated-pit endocytosis; the amino-terminus of PICALM binds phosphatidyl-inositol 4,5 bisphosphate (PIP_2), while the central portion binds adaptor protein-2 (AP-2) and the carboxyl terminus binds clathrin (Meyerholz et al., 2005; Ramanan et al., 2011a). Reducing PICALM expression by siRNA leads to altered size and shape of the clathrin-coated pit (Meyerholz et al., 2005; Tebar et al., 1999). Since the AD-protective allele of rs3851179 correlates with increased PICALM expression, we considered several mechanisms whereby PICALM may modulate AD risk. First, PICALM expression modulates APP metabolism *in vitro*. Decreased PICALM expression leads to increased APP at the cell surface while increased PICALM expression leads to increased APP internalization. Since APP is metabolized in a non-amyloidogenic pathway at the cell surface but in an amyloidogenic pathway in endosomes, the effects of PICALM on APP localization lead to altered Aβ levels: PICALM knockdown reduces Aβ while PICALM overexpression increases Aβ (Xiao et al., 2012). This pathway is not consistent with our finding that the protective rs3851179 allele increases PICALM expression.

A second pathway whereby altered PICALM may alter AD risk recognizes that altered PICALM expression modulates cell surface proteins in a protein-specific fashion. For example, decreased PICALM leads to increased GluR2 which may promote excitotoxicity (Harel et al., 2011); the protective rs3851179 allele that increases PICALM expression may reduce AD risk by reducing excitotoxicity. Increased PICALM also leads to increased cell surface transferrin

and EGFR (Harel et al., 2011; Huang, Khvorova, Marshall, & Sorkin, 2004; Meyerholz et al., 2005; Tebar et al., 1999). Consistent with a critical role for PICALM in iron homeostasis, PICALM-deficient mice suffer from severe anemia and poor erythroid development and, at the cellular level, show reduced transferrin uptake; iron supplementation ameliorates some aspects of PICALM deletion (Scotland et al., 2012). Recognizing that PICALM was robustly expressed in microvessels and that PICALM expression correlated positively with microvessel mRNAs, we speculate that increased PICALM may be AD-protective by facilitating Aβ clearance across the blood brain barrier (Sagare, Bell, & Zlokovic, 2012). Overall, altered *PICALM* levels may modulate AD risk by multiple mechanisms and is the subject of ongoing investigation.

Multiple *PICALM* exons were spliced inefficiently in human brain. Isoforms lacking many of these exons are likely to encode PICALM with altered function. Isoforms lacking exon 13 were especially common. Since a critical AP-2 binding DPF peptide motif is encoded by exon 13, the loss of exon 13 is expected to reduce AP-2 binding (Meyerholz et al., 2005). Loss of this DPF motif may be compensated by the DIF and/or FESVF motifs encoded within exons 12 and 14, respectively (Meyerholz et al., 2005). Isoforms lacking exons 13 and 14 were also detected that would lack both the DPF and FESVF motifs and would be expected to have particularly low AP-2 binding. Rare isoforms also showed an absence of exons 2 or 2-4. Since exon 2 is 143 bp, isoforms lacking exon 2 undergo a codon frameshift such that *D2-PICALM* and *D2-4-PICALM* are predicted to encode only an amino terminal PICALM fragment. Since the exon 5 SNP, rs592297, was associated with exon 2 splicing, we sought to evaluate whether this SNP was associated with AD. Although rs592297 was not available in data from Naj et al, rs1237230 is highly linked with rs592297 (r^2=0.95 in Europeans, (http://www.broadinstitute.org/mpg/snap/ldsearch.php) and is present in this dataset. Rs1237230 was modestly associated with AD (p=0.018), relative to rs3851179 (p=0.00015) (Naj et al., 2011). Hence, rs592297 does not appear to be robustly associated with AD risk relative to the primary *PICALM* SNP.

Although rs592297 may be a functional SNP in modulating exon 2-4 splicing, the modest proportion of *PICALM* present in this isoform may mitigate the SNP effects on overall PICALM function.

Conclusion

In summary, our primary findings are that multiple *PICALM* isoforms are expressed in human brain, with prominent presence in microvessels, and that overall *PICALM* expression is correlated with the AD SNP rs3851179. Rare *PICALM* isoforms are associated with AD status and / or rs592297, a SNP that is in moderate linkage disequilibrium with rs3851179. The rarity of these isoforms and their lack of association with rs3851179 suggest they are unlikely to contribute to AD risk. Since *D13-PICALM* is the most abundant PICALM isoform, future studies of PICALM function may wish to evaluate this isoform.

Acknowledgements: Parts of this chapter have previously published in Parikh, Fardo, & Estus, 2014

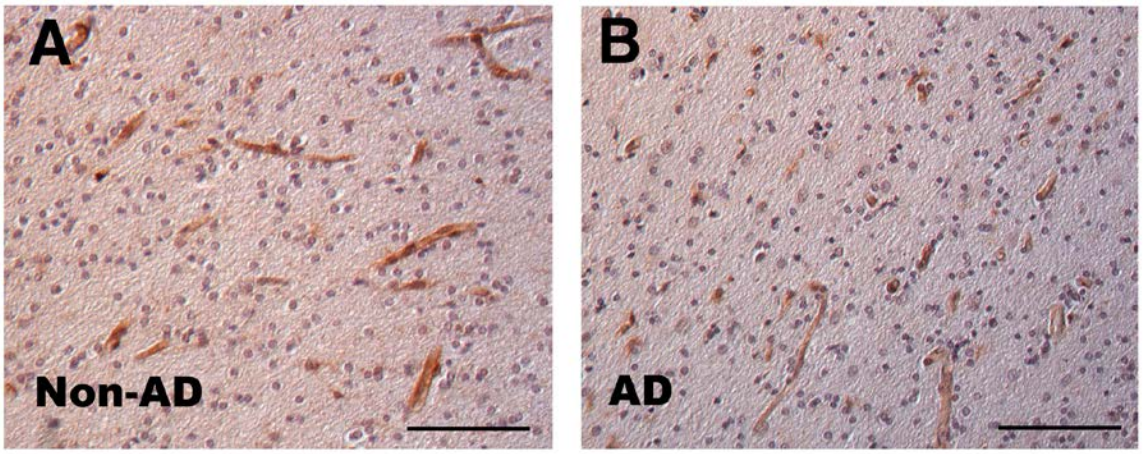

Figure 2.1 PICALM immunohistochemistry in human brain.

Human anterior cingulate was immunostained with anti-CALM antibody, revealing robust microvessel labeling (bar=100µm).

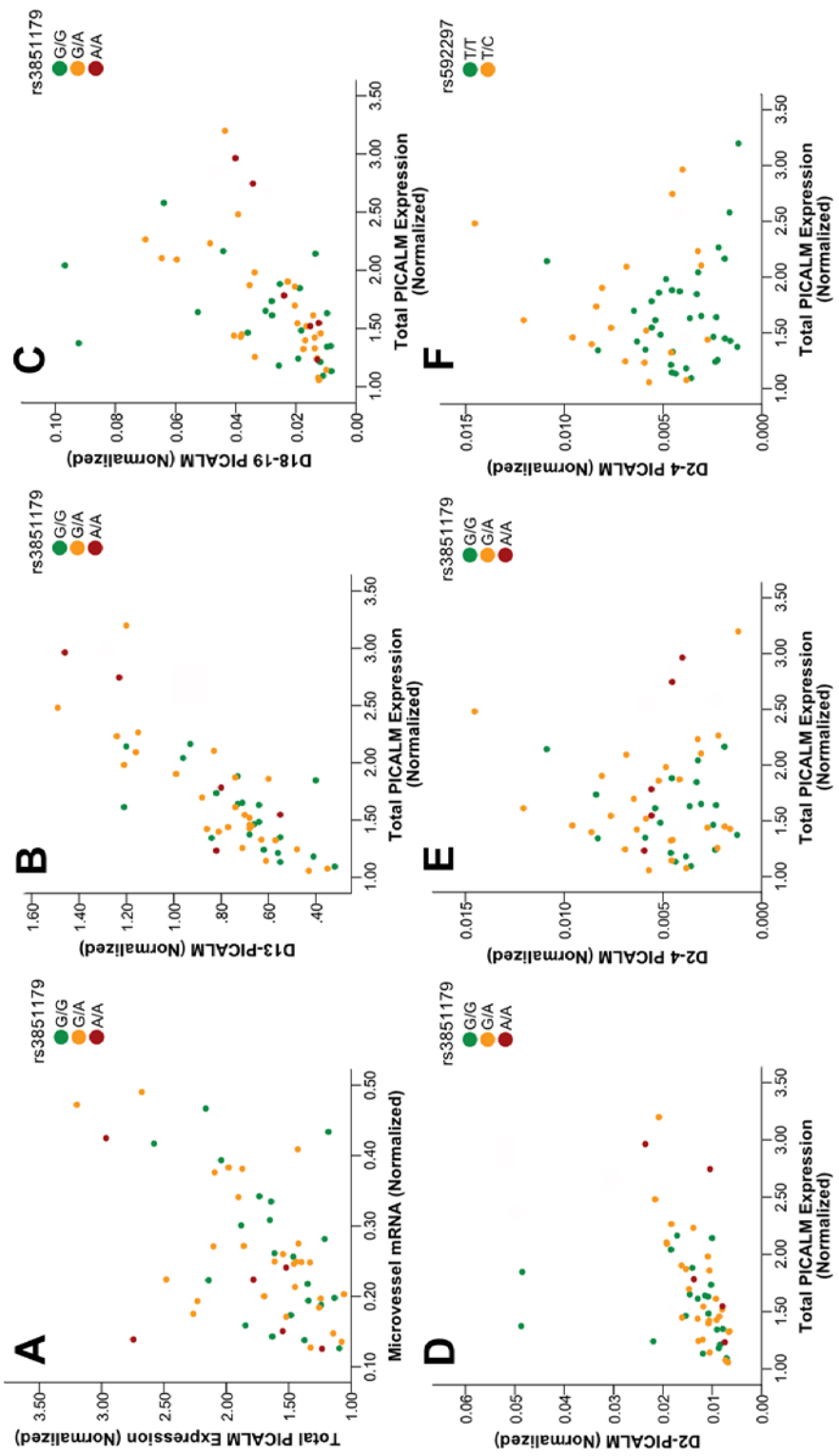
A
B
C
D
E
F
rs3851179
G/G
G/A
A/A
rs592297
T/T
T/C
Total PICALM Expression (Normalized)
Microvessel mRNA (Normalized)
D13-PICALM (Normalized)
D18-19 PICALM (Normalized)
D2-PICALM (Normalized)
D2-4 PICALM (Normalized)

Figure 2.2 Quantitative analysis of *PICALM* isoform expression.

The indicated mRNAs or isoforms was quantified by qPCR and compared relative to the AD-associated SNP rs3851179 (A-E) or rs592297, an exon 5 SNP (F).

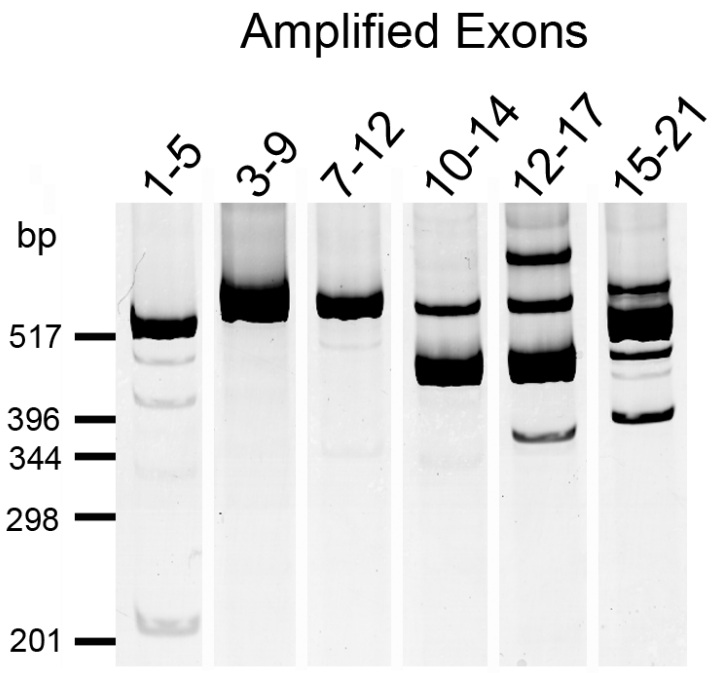

Figure 2.3 *PICALM* splice patterns in human brain.

PCR amplification across the indicated exons was performed on cDNA pooled from AD and non-AD brain samples. The products were separated by polyacrylamide gel electrophoresis and visualized by SYBR-Gold fluorescence. Single PCR products from amplifications between exon 3-9 and 7-12 indicate that individual exons between 5-11 are included with high efficiency. The presence of multiple products in other lanes represents inefficiently spliced exons as confirmed in Table 2.3.

Table 2.1 PCR Primers.

Target	Name		Sequence (5'-3')
Exons 1-5	1F	Sense	CTGACGGACCGAATCACTG
	5R	Antisense	TCAAGAAGTGCATCCATCTGA
Exons 3-9	3F	Sense	TGGCTTCAAGAAACACGTTG
	9R	Antisense	GCTTGCAGCTGTAGAATCTTTG
Exons 7-12	7F	Sense	TGAAAAAGAACCAATGCAAAGA
	12R	Antisense	CCCCATGTACTTGCTACCTGA
Exons 10-14	10F	Sense	CTTTCCAATGCAGTGTCTTCC
	14R	Antisense	CCCCAGAATCTACTACAATAACATTTG
Exons 12-17	12F	Sense	GCCCAATGATCTGCTTGATT
	17R	Antisense	CATTGTTGCAGCATTCCAAG
Exons 15-20	15F	Sense	GCTTTGATGAACTAGGTGGACTT
	20R	Antisense	GCAGTTTGGATTTTGCTGGA
Total PICALM	9	Sense	ACAGGCCCCTAGCAGTCTTC
	10	Antisense	TGCTTTTCCCTTTCATCCAC
D13	11	Sense	TGCAGCCTCTCCTGTATCCACCT
	12-14 Junction	Antisense	GGAGAAGGAGTGAATCCTCCC
D18-19	17	Sense	TGGAGTCAACCAGGTGAAAA
	17-20 Junction	Antisense	CATTTGTGGAGGCATTGTTG
D2	1	Sense	GAGGAGCTGCAGAGATGTCC
	1-3 Junction	Antisense	TACTGAATAAAACGAGTCCAGGTG
D2-4	1-5 Junction	Sense	AAAGCACCTGGACTGGCTGA
	6	Antisense	GGCAGCATTTATTACCCCATT
CD31	CD31F	Sense	ATTGCAGTGGTTATCATCGGAGT
	CD31R	Antisense	CTCGTTGTTGGAGTTCAGAAGTGG
VWF	vWF F	Sense	CGGCTTGCACCATTCAGCTA
	vWF R	Antisense	TGCAGAAGTGAGTATCACAGCCATC
Exon12-20	12	Sense	GCCCAATGATCTGCTTGATT
	20	Antisense	TTGGTTGCGTCATTACAGGA
GFAP	Ex 4	Sense	AAGAGATCCGCACGCAGTAT
	Ex 5	Antisense	GTAGTCGTTGGCTTCGTGCT
SYN	SYN F	Sense	AGGGAACACATGCAAGGAG
	SYN R	Antisense	CCTTAAACACGAACCACAGG

PCR primers used for screening splice variants, cloning, qPCR and sequencing.

Table 2.2 Multivariate Linear Regression Analysis of Total *PICALM* and Isoforms.

	Standardized β Coefficients	**p-value**
Model: Total PICALM Expression (Adj r^2=0.46)		
AD Status	-0.05	0.66
Rs3851179	0.298	6.9×10^{-3}
Microvessel mRNA	0.387	8.6×10^{-4}
SYP mRNA	-0.455	1.2×10^{-4}
GFAP mRNA	0.313	0.01
Model: D13-PICALM (Adj r^2=0.54)		
AD Status	-0.304	4.9×10^{-3}
Rs3851179	0.268	8.1×10^{-3}
Microvessel mRNA	0.302	4.0×10^{-3}
SYP mRNA	-0.519	4.2×10^{-6}
GFAP mRNA	0.513	1.8×10^{-5}
Model: D18-19 PICALM (Adj r^2=0.21)		
AD Status	0.011	0.94
Rs3851179	-0.036	0.78
Microvessel mRNA	0.255	0.06
SYP mRNA	-0.36	8.0×10^{-3}
GFAP mRNA	0.312	0.03

Table 2.2, continued.

Model: D2-PICALM (Adj r^2=0.41)		
AD Status	0.238	0.05
Rs3851179	0.084	0.46
Microvessel mRNA	0.287	0.02
SYP mRNA	-0.429	1.0×10^{-3}
GFAP mRNA	0.24	0.06
Model: D2-4 PICALM (Adj r^2=0.10)		
AD Status	-0.322	0.03
Rs3851179	0.114	0.40
Microvessel mRNA	0.002	0.99
SYP mRNA	0.233	0.10
GFAP mRNA	-0.041	0.79
Model: D2-4 PICALM (Adj r^2=0.24)		
AD Status	-0.245	0.08
Rs592297	0.384	4.0×10^{-3}
Microvessel mRNA	0.004	0.97
SYP mRNA	0.243	0.06
GFAP mRNA	0.001	0.99

Total *PICALM, D13-PICALM, D18-19 PICALM, D2-PICALM*, and *D2-4 PICALM* expression was analyzed as a function of AD, rs3851179 and microvessel mRNA, *SYP* and *GFAP* content by using a linear regression model. *D2-4 PICALM* was also analyzed as a function of rs592297, along with AD, microvessel mRNA, *SYP* and *GFAP*. Adj: Adjusted

Table 2.3 Semi-Quantitative *PICALM* Isoform Analysis.

	Rs3851179 Genotype	
PICALM Isoforms (exons 12-20)	AA (%Total Clones)	GG (%Total Clones)
D13	45.4 ± 5.3	44.0 ± 9.0
D13, 14	1.9 ± 1.6	1.7 ± 1.6
Dp15	1.8 ± 2.2	4.5 ± 4.4
D13, p15	15.3 ± 0.5	16.4 ± 3.2
D13, 18	9.2 ± 4.3	9.3 ± 1.5
D13, p15, 18	5.9 ± 1.8	4.2 ± 0.7
D18	2.8 ± 2.1	3.1 ± 1.8
D13, 18, 19	2.6 ± 2.6	0.9 ± 0.4
D13, p15, 18, 19	3.7 ± 3.3	0.4 ± 0.4
Full Length (12-20)	7.2 ± 3.0	12.6 ± 6.5

Complementary DNA from three rs3851179A/A and three G/G samples was amplified and the PCR amplicons cloned. A total of 847 random clones were then sequenced. This table shows the frequencies of each isoform (mean ± SD), noting that “D” indicates that an exon is missing while “p” designates a partial exon deletion, i.e., p15 refers to clones lacking first 15 bp of exon 15. Additional isoforms with an average frequency of less than 1% are not included, including rare isoforms that lacked the first 21 bp of exon 13.

Chapter 3
An Intronic PICALM Polymorphism, rs588076, is Associated with Allelic Expression of a PICALM Isoform

Abstract

Although genome wide studies have associated single nucleotide polymorphisms (SNP)s near *PICALM* with Alzheimer´s disease (AD), the mechanism underlying this association is unclear. PICALM is involved in clathrin-mediated endocytosis and modulates Aβ clearance *in vitro*. Comparing allelic expression provides the means to detect cis-acting regulatory polymorphisms. Thus, we evaluated whether PICALM showed allele expression imbalance (AEI) and whether this imbalance was associated with the AD-associated polymorphism, rs3851179.

We measured *PICALM* allelic expression in 42 human brain samples by using next-generation sequencing. Overall, *PICALM* demonstrated equal allelic expression with no detectable influence by rs3851179. A single sample demonstrated robust global *PICALM* allelic expression imbalance (AEI), i.e., each of the measured isoforms showed AEI. Moreover, the *PICALM* isoform lacking exons 18 and 19 (*D18-19 PICALM*) showed significant AEI in a subset of individuals. Sequencing these individuals and subsequent genotyping revealed that rs588076, located in *PICALM* intron 17, was robustly associated with this imbalance in *D18-19 PICALM* allelic expression ($p=9.54 \times 10^{-5}$). This polymorphism has been associated previously with systolic blood pressure response to calcium channel blocking agents. To evaluate whether this polymorphism was associated with AD, we genotyped 3269 individuals and found that rs588076 was modestly associated with AD. However, when both the primary AD SNP rs3851179 was added to the logistic regression model, only rs3851179 was significantly associated with AD.

PICALM expression shows no evidence of AEI associated with rs3851179. Robust global AEI was detected in one sample, suggesting the existence of a rare SNP that strongly modulates *PICALM* expression. AEI was detected for the *D18-19 PICALM* isoform, and rs588076 was associated with this

AEI pattern. Conditional on rs3851179, rs588076 was not associated with AD risk, suggesting that *D18-19 PICALM* is not critical in AD. In summary, this analysis of *PICALM* allelic expression provides novel insights into the genetics of *PICALM* expression and AD risk.

Introduction

Phosphatidylinositol binding clathrin assembly protein (*PICALM*) facilitates clathrin-mediated endocytosis. PICALM binds phosphatidylinositol 4,5-bisphosphate (PIP_2), adaptor protein 2 (AP_2) and clathrin to mediate endocytic clathrin coated vesicle formation at the plasma membrane. Although PICALM is ubiquitously expressed, PICALM expression is more pronounced in microvessels (Baig et al., 2010; Parikh, Fardo, et al., 2014). Previous studies have shown PICALM co-localizes with APP and modulates amyloid beta (Aβ) generation (D'Angelo et al., 2013; Kanatsu et al., 2014; Xiao et al., 2012). Accumulation of Aβ deposits is a hallmark of Alzheimer's Disease (AD) pathology.

Genome wide association studies in multiple cohorts have identified single nucleotide polymorphisms (SNP)s near the *PICALM* gene as significantly associated with AD risk (Harold et al., 2009; Jun et al., 2010; Lambert et al., 2009; Pedraza et al., 2014; Seshadri et al., 2010). Studies were first conducted with Caucasian populations and then independently verified in several although not all Asian populations (Chen et al., 2012; Li et al., 2011; G. Liu et al., 2013; Miyashita et al., 2013; Yu et al., 2011). These studies report that the rs3851179 A allele reduces AD risk with an odds ratio of 0.88 (Harold et al., 2009). This SNP is located approximately 80kb 5' of *PICALM.*

Understanding how rs3851179 alters *PICALM* to impact AD risk may lead to novel insights into AD mechanisms and potential treatments. Since rs3851179

is not in linkage disequilibrium (LD) with a SNP that alters a *PICALM* amino acid (r^2<0.1), we hypothesize that rs3851179 is associated with changes in mRNA transcription or processing. Allelic expression imbalance (AEI) which is an expression difference between allelic transcripts within an individual, has been used to detect *cis*-regulatory effects (Jentarra, Rice, Olfers, Saffen, & Narayanan, 2011; Jones & Swallow, 2011; Mondal, Sharma, Elbein, & Das, 2013; Pham et al., 2012; Smith et al., 2013).

Here, we performed an AEI analysis by comparing allelic expression through the use of two exonic SNPs, rs76719109 and rs592297, in AD and non-AD brain samples. These studies included 35 samples that were heterozygous for rs76719109 and 19 samples that were heterozygous for rs592297. While *PICALM* expression did not show AEI overall, one individual showed robust *PICALM* AEI, with an allelic ratio of 0.76. Additionally, significant AEI was detected for the *PICALM* isoform lacking exons 18 and 19 (*D18-19 PICALM*). Sequencing and additional genotyping established that rs588076 was robustly associated with this AEI pattern. Interestingly, rs588076 has been associated with blood pressure response to Ca++ channel blocking agents (Kamide et al., 2013). We discuss these overall results in the context that genetic regulation of *PICALM* isoforms relative to AD risk is highly complex with further work necessary to elucidate the mechanisms modulating genetic risk.

Materials and Methods

DNA and RNA extraction from human brain tissue

The RNA and DNA samples for this study were from de-identified AD and non-AD human brain anterior cingulate specimens provided by the University of Kentucky AD Center Neuropathology Core and have been described previously (Ling et al., 2012; Malik et al., 2013; Parikh, Fardo, et al., 2014). The overall dataset included 30 AD samples (14 male, 16 female) and 30 non-AD samples

(15 male, 15 female). The age at death for individuals that were cognitively intact, i.e., non-AD, was 82 ± 8 years (mean ± SD, n = 30) while age at death for AD individuals was 82 ± 6 (n = 30). The average post-mortem interval (PMI) for non-AD individuals was 2.8 ± 0.9 hours (mean ± SD, n = 30) while the PMI for AD individuals was similar at 3.4 ± 0.6 hours (n = 30). For the rs76719109 AEI assay, a subset of 35 samples were heterozygous for this SNP and included 18 non-AD (9 male, 9 female) and 17 AD (9 male, 8 female) (Table 3.1, 3.2). For the rs592297 AEI assay, a total of 19 out of 60 samples were heterozygous, 13 non-AD (7 male, 6 female) and 6 AD (3 male, 3 female) (Table 3.3, 3.4). Preparation of gDNA, RNA and cDNA was performed as described in previous studies (Ling et al., 2012; Malik et al., 2013; Parikh, Fardo, et al., 2014). Although RNA integrity analyses were not performed prior to reverse transcription, others have demonstrated that for qPCR with short amplicons, normalized expression differences are comparable between samples with moderate RNA degradation and those with high integrity RNA (Fleige & Pfaffl, 2006). We recognize that the absence of RNA integrity analysis constitutes a caveat of this study.

Genotyping and sequencing

DNA samples were genotyped for rs3851179, rs76719109, rs592297 and rs588076 by using unlabeled PCR primers and two allele-specific TaqMan FAM and VIC dye-labeled MGB probes (Pre-designed TaqMan SNP Genotyping Assay, Applied Biosystems) on a real-time PCR machine (Chromo4, MJ Research PTC-200).

Allelic imbalance assay

Rs76719109 is in exon 17. For AEI analysis with rs76719109, *PICALM* was amplified from exon 17 to exon 20 for cDNA and exon 17 to intron 17 for genomic DNA. For rs592297, *PICALM* was amplified from exon 5 to exon 6 for cDNA and exon 5 to intron 5 for genomic DNA. Exon numbering is according to *PICALM*-005 ENST00000393346 for exons 1-16 and exons 17-21 correspond to

the final five exons within *PICALM*-002 ENST00000532317 in Ensembl, since no single ENSEMBL transcript includes each of the exons the we identify here (Paul Flicek). The PCR primers included Ion Torrent adapters, individual barcodes and DNA sequence flanking the region of interest (Table 3.5). Each PCR reaction (50uL) contained 1x PCR buffer, 20ng cDNA or 100 ng gDNA, 1uM of forward and reverse primer, 0.1mM dNTP and 0.5 Units Taq (Platinium Taq, Invitrogen). Cycles consisted of pre-incubation at 95˚C for 2 minutes, followed by 28 cycles of 95˚C for 15 s, 60˚C for 30s and 72˚C for 60s followed by incubation at 75˚C for 7 minutes. To acquire equal representation from each sample, relative amounts of PCR product were quantified by subjecting 10 uL of PCR product to electrophoresis on 7.5% polyacrylamide gels and SYBR gold staining relative to a Low DNA Mass Ladder (Invitrogen). Approximately 2 ng of each individual's cDNA and gDNA PCR products were pooled, purified using Agencourt AMPure XP and subjected to Ion Torrent sequencing on a Ion Torrent 316 chip (Ion PGM Sequencer).

Data extraction and analysis of allelic mRNA expression

Allelic counts were extracted from DNA sequences by using Perlscript in a three-step fashion: (i) sequences corresponding to each sample were separated based on their barcode, (ii) gDNA and cDNA were then separated based on the presence of intronic and exonic sequences, respectively, and (iii) allele counts were obtained by using sequences that bridged the SNP of interest.

Standard curve generation

One rs76719109 homozygous major (GG) and one homozygous minor (TT) individual was selected based on similar qPCR copy numbers. Five dilutions were prepared with different ratios of each individual's cDNA: 1:4, 1:2, 1:1, 2:1, and 4:1. These samples were PCR amplified and subjected to sequencing as described above.

Statistical analysis

Analysis of allelic counts was based upon the assumption that transcript read counts follow a Poisson distribution (H. Jiang & Wong, 2009). As such, each allele from the heterozygous SNP was used to define two random variables. Following the rs76719109 example of a G/T SNP, we denote the pair of transcript counts as $G \sim Poisson\,(\lambda_G)$ and $T \sim Poisson\,(\lambda_T)$. That is, G and T are Poisson-distributed random variables with means λ_G and λ_T, respectively. It can then be readily shown that for a given pair of realized transcripts counts, G=g and T=t, the transcript count of either allele is binomially distributed with success probability equal to a ratio of component means. That is, $G \mid G + T = g + t \sim Bin\,(g + t, p = \frac{\lambda_G}{\lambda_G + \lambda_T})$. Testing for AEI then simplifies to an examination of the null hypothesis that the pair of transcript counts comes from the same distribution, i.e., that $\lambda_G = \lambda_T$, which is equivalent to testing $H_0: p = \frac{1}{2}\,[G \mid G + T = g + t \sim Bin\,(g + t, \frac{1}{2})]$. This null hypothesis agrees with the intuition that when the total of transcript counts is known, the number generated from a specific allele is essentially a sequence of independent, equally probable trials. Thus, rejection of this null hypothesis corresponds to AEI.

Measuring transcripts from genomic DNA is one way of correcting for the possibility of differential experimental error between allele transcript counts. Conceptually, one could adapt methods for determining AEI by an appropriate adjustment with the ratio of reads from gDNA as these reads should theoretically come from the same distribution regardless of AEI (Fardo et al., unpublished). Alternatively, it can be assumed that one allele is derived from a distribution with an inflated mean solely due to experimental error (i.e., under the null hypothesis of no AEI). In this case, we have that the means of the transcript reads satisfy either $\lambda_G = (1 + \delta)\lambda_T$ or $(1 + \delta)\lambda_G = \lambda_T$. Here, the probability parameter, p, for

the count probability in the AEI test becomes $\frac{1+\delta}{2+\delta}$ or $\frac{1}{2+\delta}$, respectively. For our gDNA data, we have a maximum 8.5% increase of one allele over the other and chose to conservatively assume a 20% mean increase (i.e., $\delta = 0.2$). We then calculate the AEI test p-value from the lesser-significant test of $H_0: p = \frac{1+\delta}{2+\delta}$ and $p = \frac{1}{2+\delta}$.

Genotype association with AD risk

The Mayo Clinic dataset has been described previously (Naj et al., 2011; Ridge, Mukherjee, Crane, Kauwe, & Alzheimer's Disease Genetics, 2013). Briefly, the Mayo Clinic dataset contained 1789 cases and 2529 non-ADs collected from six centers from the US and Europe as described (Naj et al., 2011). Direct genotyping of rs3851179 and rs588076 was performed using a TaqMan SNP genotyping assay in an ABI PRISM 7900HT Sequence Detection System with 384-well block module from Applied Biosystems (California, USA). First-pass genotype cluster calling was analyzed using the SDS software version 2.2.3 (Applied Biosystems, California, USA). Variants passed Hardy-Weinburg (P>0.05) and minor allele frequencies are consistent with public databases (EVS, HapMap, 1000G). Association testing for rs3851179, with and without rs588076, was carried out in PLINK (Purcell et al., 2007) by using an additive logistic regression model corrected for appropriate covariates; diagnosis age, *APOE* ε4, APOE ε2, sex and contributing center.

Results

To detect the presence of regulatory cis-acting SNPs in human brain samples, we measured allelic ratios in cDNA from reverse transcribed mRNA. Heterozygosity for an exonic “reporter” SNP provides the means to compare the expression of one allele with another allele within an individual. Our criteria for reporter SNPs for AEI analysis is that the SNPs are present in exons and have a

minor allele frequency (MAF) greater than 15%, which allows for sufficient sample numbers for analysis. Only two PICALM SNPs satisfied these criteria, rs76719109 and rs592297 (**Figure 3.1**). Rs76719109 has a MAF of 0.44 and resides within exon 17; PCR amplification from exon 17-20 allowed us to measure AEI for total *PICALM* as well as *PICALM* splice variants lacking exon 18 or exons 18-19 (**Figure 3.1a**). Rs592297 has a MAF of 0.20 and resides in exon 5. PCR amplification from exon 5-6 produced a single PCR product for cDNA (**Figure 3.1b**). The AEI assay was validated in two ways. First, we tested the linearity of the assay by generating a cDNA standard curve consisting of five different rs76719109 T:G ratios (**Figure 3.2**). Our input T:G ratios ranged from 1:4 to 4:1. We found a robust linear relationship between input and observed T:G ratios. Second, we applied our experimental approach to gDNA, which represented a positive control with an expected "allelic" ratio of 1.0. Rs76719109 and rs592297 showed gDNA ratios of 1.01 ± 0.03 (mean ± SD, n=35) and 0.96 ± 0.05 (mean ± SD, n=19), respectively (**Figure 3.3**). Hence, this AEI assay appears robust for detecting and quantifying variations in allelic expression.

To evaluate whether the AD-associated SNP rs3851179 was associated with unequal allelic *PICALM* expression, we performed AEI analysis with rs76719109 and rs592297on a total of 54 samples. Twelve of these 54 samples were heterozygous for both SNPs. Hence, we analyzed *PICALM* for AEI in a total of 42 unique individual samples. This effort analyzed 4.2 million sequences for rs76719109 and 1.4 million sequences for rs592297. If rs3851179 modulated total *PICALM* expression, we expected to see significant AEI in individuals heterozygous for rs3851179, but not in individuals homozygous for rs3851179. When we analyzed the results for the exon 17 SNP, rs76719109, significant AEI was observed in only a single sample, termed AD40 (see below). To evaluate whether a subtle difference in allelic expression may be present and associated with rs3851179, we compared the mean allelic expression between the rs3851179 homozygous and heterozygous groups. This approach did not

discern a significant difference between the two groups, i.e., the allelic ratios for rs3851179 homozygous and heterozygous groups was 0.94 ± 0.08 (n=17) and 0.97 ± 0.06 (n=18), respectively (**Figure 3.4a**, p= 0.24, t-test). Hence, rs3851179 did not appear associated with PICALM AEI. To confirm this finding and extend the analysis to additional samples, we analyzed allelic expression by using the exon 5 SNP, rs592297. Significant AEI was not observed in any sample, noting that the sample with the significant AEI result from the rs76719109 analysis was homozygous for rs592297 and not suitable for evaluation. When the allelic ratios were analyzed by t-test to evaluate whether rs3851179 was associated with allelic expression, the findings confirmed that rs3851179 was not associated with robust AEI; the allelic ratios were 0.93 ± 0.05 (n= 4) for rs3851179 homozygotes and 1.01 ± 0.07 (n= 15) for heterozygotes (**Figure 3.4b**, p= 0.06). Hence, we found that the total *PICALM* allelic ratio for each person was remarkably consistent with both reporter SNPs; rs3851179 is not associated with overall allelic *PICALM* expression.

Interestingly, cDNA from the individual termed AD40 showed significant unequal allelic mRNA expression with a T:G ratio of 0.76 (**Figure 3.4a**, Table 3.6). This ratio is based on a total of four experiments that detected a total of 68141 copies of the T allele and 88400 copies of the G allele. This AEI was not due to genomic normalization as the genomic T:G ratio was 1.01. These data are based upon the rs76719109 SNP because this individual was homozygous for rs592297. A similar result was obtained when each of four separate replicates were analyzed individually, i.e., when each replicate was analyzed individually, the T:G ratio was 0.73 ± 0.04 (mean ± SD). Hence, significant AEI was observed in a single individual among the 42 unique samples.

Having considered overall *PICALM* allelic expression, we proceeded to apply this AEI analysis to *PICALM* isoforms. The exon 17 to exon 20 PCR

amplicons captured three different *PICALM* isoforms because exons 18 and 19 are variably spliced. These isoforms were termed *full length PICALM* (contains exons 18-19), *D18-PICALM* (lacked exon 18) or *D18-19 PICALM* (lacked both exons 18 and 19). We analyzed each of these isoforms for the presence of AEI as a function of rs3851179 heterozygosity. For the full length PICALM and D18-PICALM isoforms, significant AEI was observed only in the AD40 sample. To evaluate whether a subtle difference in allelic expression may be present, we compared the allelic expression of the *full length PICALM* isoform between the rs3851179 homozygous and heterozygous groups by using a t-test. However, no difference was observed as the average T:G ratio in the rs3851179 homozygous and heterozygous groups was 0.93 ± 0.07 (n=17) and 0.93 ± 0.06 (n=18), respectively (**Figure 3.5a**, p= 0.81). Likewise, for the *D18-PICALM* isoform, the rs3851179 homozygous and heterozygous groups showed mean T:G ratios of 0.95 ± 0.09 (n=17) and 1.01 ± 0.12 (n=18), respectively (**Figure 3.5b**, p=value= 0.13). When we evaluated the D18-19 PICALM isoform, significant AEI was detected in multiple samples (**Figure 3.5c**). We analyzed these results in two ways. First, we compared the frequency of samples with significant AEI between the rs3851179 homozygous and heterozygous individuals by using a Fisher's exact test; a significant difference between groups was not detected (**Figure 3.5c**, p= 0.44). Second, we compared the mean T:G ratio between rs3851179 homozygous and heterozygous individuals by using a t-test. However, the rs3851179 homozygous and heterozygous individuals showed similar values that did not achieve significance , i.e., 1.19 ± 0.16 and 1.11 ± 0.22, respectively (p=0.08). Hence, rs3851179 heterozygosity was not associated with AEI for these *PICALM* isoforms.

We considered the subset of samples that showed significant AEI further. Among these, AD40 showed significant AEI for each of the isoforms, with the *D18, D18-19* and *full length PICALM* isoforms having allelic T:G ratios of 0.77, 0.53 and 0.77, respectively. As noted above, this finding is consistent with the

hypothesis that a rare SNP acts to alter global *PICALM* allelic expression in this individual. Additionally, we noted that the *D18-19 PICALM* isoform showed significant AEI for multiple individuals (**Figure 3.5c**). In these eight individuals, the rs76719109T allele was expressed more than the G allele with the ratio ranging from 1.30 to 1.48 (Table 3.7). This is in contrast to AD40 where the T allele was expressed less than G allele at a ratio of 0.53 (Table 3.6, 3.7).

Since the *D18-19 PICALM* isoform but not overall PICALM showed AEI in multiple samples, we hypothesized that a local SNP influences this splice pattern. To identify this SNP, we sequenced 6400 bp of genomic DNA between exons 17-20 in C11 and AD33, the two individuals showing the highest AEI ratio (Table 3.1). We identified several SNPs that were heterozygous in these samples including rs588076, rs645299, and rs618629. The MAF for these SNPs in CEU range from 20-31% (Table 3.8). Additionally, these SNPs are in strong LD with each other (Table 3.8). Rs588076 and rs618629 reside in intron 17 while rs645299 is within intron 18. We genotyped all samples for rs588076. The frequency of samples showing significant AEI was significantly associated with rs588076 heterozygosity (**Figure 3.5d**, $p=9.54 \times 10^{-5}$, Fisher's exact test). We interpret these results as strongly suggesting that rs588076, or a SNP in strong LD with rs588076, is functional by modulating *PICALM* exon 18-19 splicing.

Since rs588076 is associated with *D18-19 PICALM* AEI and rs3851179 has been robustly associated with AD, we evaluated the extent that rs588076 is associated with AD risk. We evaluated 1789 AD and 2529 non-AD individuals from the Mayo Clinic cohort. Rs588076 was significantly associated with AD risk when analyzed in a logistic regression model (odds ratio = 0.8413, 95% confidence intervals (0.7151-0.9898), p=0.0372). However, when rs3851179 was added to this logistic regression model, only rs3851179 was significantly associated with AD (Table 3.9). Haplotypic analysis confirmed that the haplotype

containing both rs588076 and rs3851179 report the same association with AD as the haplotype containing only rs3851179 (data not shown). Hence, rs588076 is associated with *D18-19 PICALM* AEI but not AD risk.

Discussion

The primary findings of this report include (i) overall *PICALM* expression shows no evidence of global AEI even when parsed by AD-associated SNPs, (ii) robust global AEI was detected in one sample, suggesting the existence of a rare SNP that strongly modulates *PICALM* expression, and (iii) eight individuals show AEI for the *D18-19 PICALM* isoform that is associated with rs588076. However, rs588076 was not associated with AD risk when considered in a model that also included rs3851179. In summary, analysis of allelic expression has proved a useful tool for the evaluation of cis-acting regulatory polymorphisms and AD risk.

A consistent pattern of AEI in overall *PICALM* expression was not detected. This was unexpected since Xu et al reported consistent and robust *PICALM* AEI (X. Xu et al., 2011). The reason for different results in these two studies is unclear. The studies are similar in that both used rs76719109 as a reporter SNP and similar although not identical PCR primers. The studies differ in that Xu et al used an Asian population while this report studied Caucasians. One explanation that would account for the difference in the studies was the presence of a confounding SNP in the Asian population in the genomic primer sequence because much of the AEI in Xu et al. was due to correction for imbalance in gDNA (X. Xu et al., 2011), although such a SNP has not yet been reported.

We previously reported that the AD-associated SNP rs3851179 was associated with a modest difference in *PICALM* expression when analyzed relative to cell-type specific mRNAs; the minor rs3851179A allele appeared to be expressed modestly higher than the G allele (Parikh, Fardo, et al., 2014). A

similar difference was not observed here. One possible interpretation of these findings is that rs3851179 or its proxy AD SNP acts in a cell-type specific fashion that was discernible in our analysis that included cell-type specific markers. The current AEI study had smaller sample size because only the samples that were heterozygous for rs76719019 or rs592297 were suitable for analysis. However, this would not be expected to affect the AEI results because they rely upon an intra-individual analysis. We interpret these results overall as suggesting that the AD-associated SNP, or its functional proxy, acts in a cell-type specific fashion to modulate *PICALM* expression. This cell-type specific action was not detectable in this AEI study of mRNA derived from multiple cell types.

The second major finding was that robust AEI was detected for all *PICALM* isoforms in one individual, arguing for the existence of a rare functional SNP that strongly modulates total *PICALM* expression. For this individual, the rs76719109G allele was consistently more abundant than the T allele for each *PICALM* isoform. We hypothesize that AD40 is unique among the 42 samples in showing AEI because this sample is heterozygous for a causal SNP. If this causal allele is present in the heterozygous state in 1 of 42 people, this SNP has a minor allele frequency of ~1.2%. Although current sequencing studies of the *PICALM* promoter region have not yet identified candidate functional SNPs for AEI in this sample, these studies are on-going and a SNP that strongly modulates *PICALM* expression would be expected to be a robust AD risk factor.

The third major finding was that the *D18-19 PICALM* isoform showed robust AEI. There was a strong skew towards increased expression of the rs76719109T allele. Sequencing identified several candidate SNPs including rs588076, which is 509 bp downstream of exon 17. This SNP was found to be robustly associated with AEI for *D18-19 PICALM*. There are three possible ways rs588076 could influence *D18-19 PICALM* splicing efficiency: (i) rs588076 is in

high LD with a functional SNP that modulates splicing, (ii) rs588076 and other SNPs influence *D18-19 PICALM* splicing in a cooperative manner, and/or (iii) rs588076 directly influences splicing. Further studies are necessary to discern among these possibilities.

The biological significance of the rs588076 association with *D18-19 PICALM* is complex. *D18-19 PICALM* transcripts account for 1-2% of total *PICALM expression* (Parikh, Fardo, et al., 2014). Thus rs588076 is significantly associated with AEI for a *PICALM* isoform that is relatively rare in brain. Exons 18 and 19 encode a total of 27 amino acids that are part of the carboxyl terminal region required for clathrin binding and endocytosis (Scotland et al., 2012). Hence, the protein encoded by *D18-19 PICALM* is likely to have reduced function (Scotland et al., 2012). However, rs588076 was not associated with AD risk and did not enhance the logistic regression model for the rs3851179 association with AD. This leads us to conclude that the rs588076 and *D18-19 PICALM* isoform may be too rare in the brain to influence AD pathogenesis. Interestingly, rs588076 was recently associated with the blood pressure response to Ca++ channel blocking agents (Kamide et al., 2013). Since rs588076 is associated only with *D18-19 PICALM*, we speculate that this isoform may be more abundant in other tissues and rs588076 actions upon *D18-19 PICALM* mediate this systolic blood pressure phenotype.

Conclusion

In summary, analysis of allelic expression has shown that compelling *PICALM* AEI was not observed in most brain RNA samples. Strong global AEI was documented in one sample, suggesting the existence of a rare *PICALM* regulatory SNP. A pattern of AEI was clearly discerned for the *D18-19 PICALM* isoform and rs588076 was significantly associated with this pattern. Rs588076 was not associated with AD risk although this SNP has been associated with a

blood pressure-related phenotype. Allele-dependent expression studies may provide further insights into additional AD-associated polymorphisms.

Acknowledgements: Parts of this chapter has previously published in Parikh, Medway, Younkin, Fardo, & Estus, 2014.

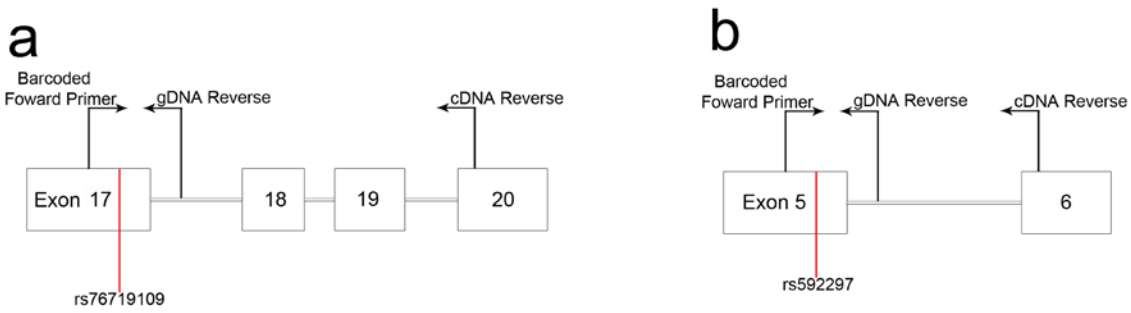

Figure 3.1 Rs76719109 and rs592297 AEI assays.

a) For the exon 17 SNP rs76719109, a barcoded forward primer was positioned in exon 17, and a reverse primer was positioned in intron 17 (genomic samples) or exon 20 (cDNA samples). b) For the exon 5 SNP rs592297 assay, a barcoded forward primer was positioned in exon 5, and a reverse primer was positioned in intron 5 (genomic samples) or exon 6 (cDNA samples).

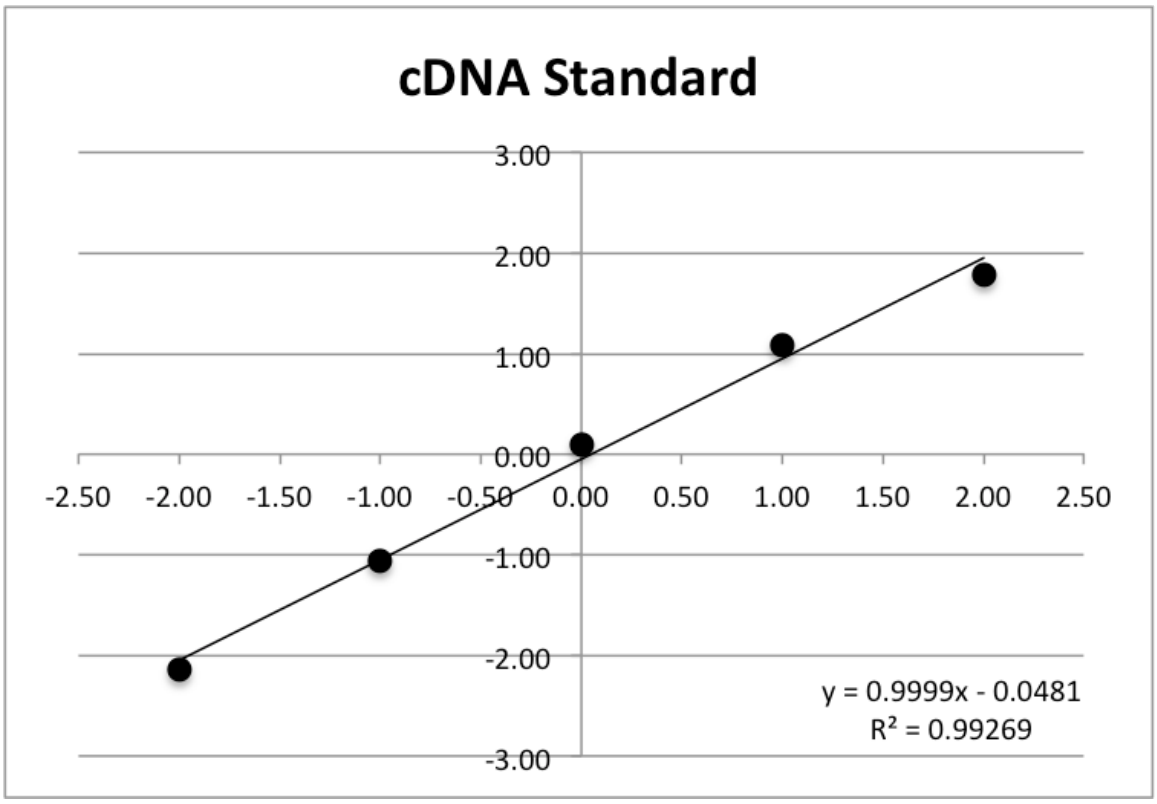

Figure 3.2 Linearity of allelic expression assay.

Different proportions of rs76719109 T and G homozygous cDNA were mixed to test the linearity of the AEI assay. The T:G ratios were 1:4, 1:2, 1:1, 2:1, and 4:1. An overall linear relationship was found (r^2=0.99). The slope was 0.999, i.e., the assay detected the T and G alleles with equal efficiency. The graphs are plotted $\log_2$ to avoid compression at the lower ratios and thereby better visualize the data (X. Xu et al., 2011).

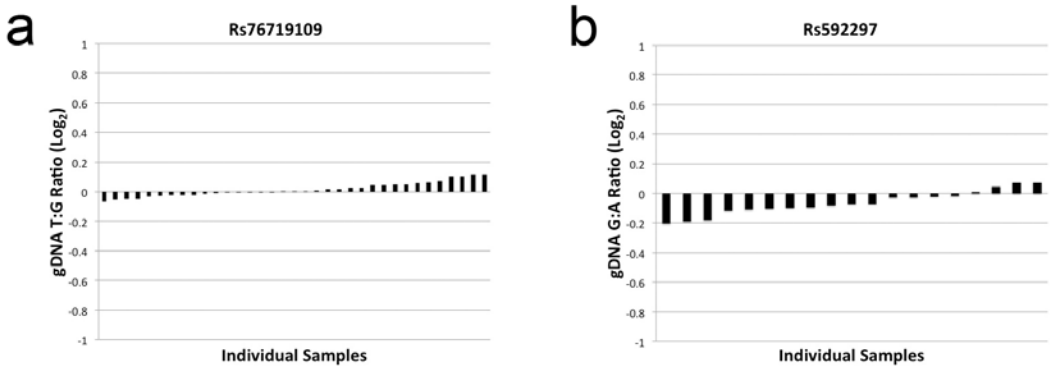

Figure 3.3 Genomic DNA Allelic Ratios.

a-b) The allelic ratio for the gDNA samples for rs76719109 and rs592297 is shown. None of the samples showed significant AEI with each of the samples consistently near the expected 1:1 ratio (note that a 1.0 ratio is equal to 0 in $\log_2$).

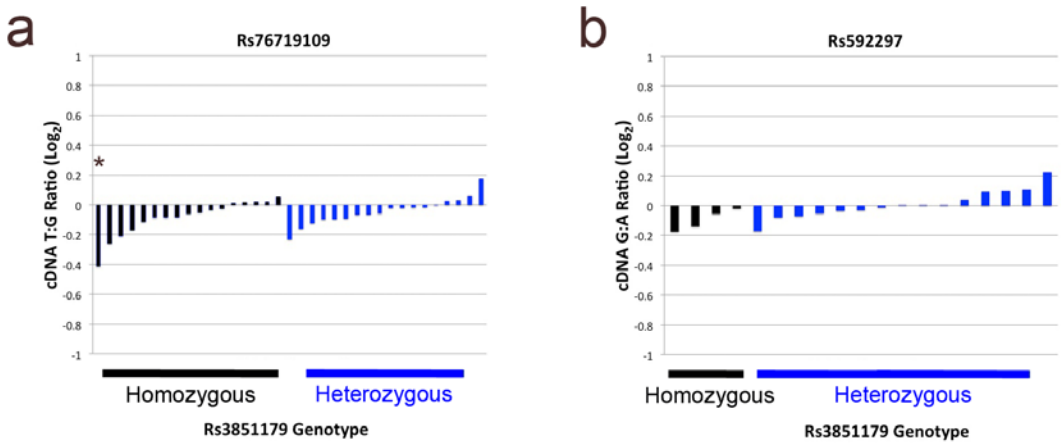

Figure 3.4 Evaluation of total *PICALM* AEI with respect to rs3851179.

a-b) Allelic *PICALM* expression was assessed by rs76719109 or rs592297. Each individual sample was normalized to its gDNA ratio. Rs3861179 was not associated with significant AEI, i.e., only one sample (*) showed significant AEI.

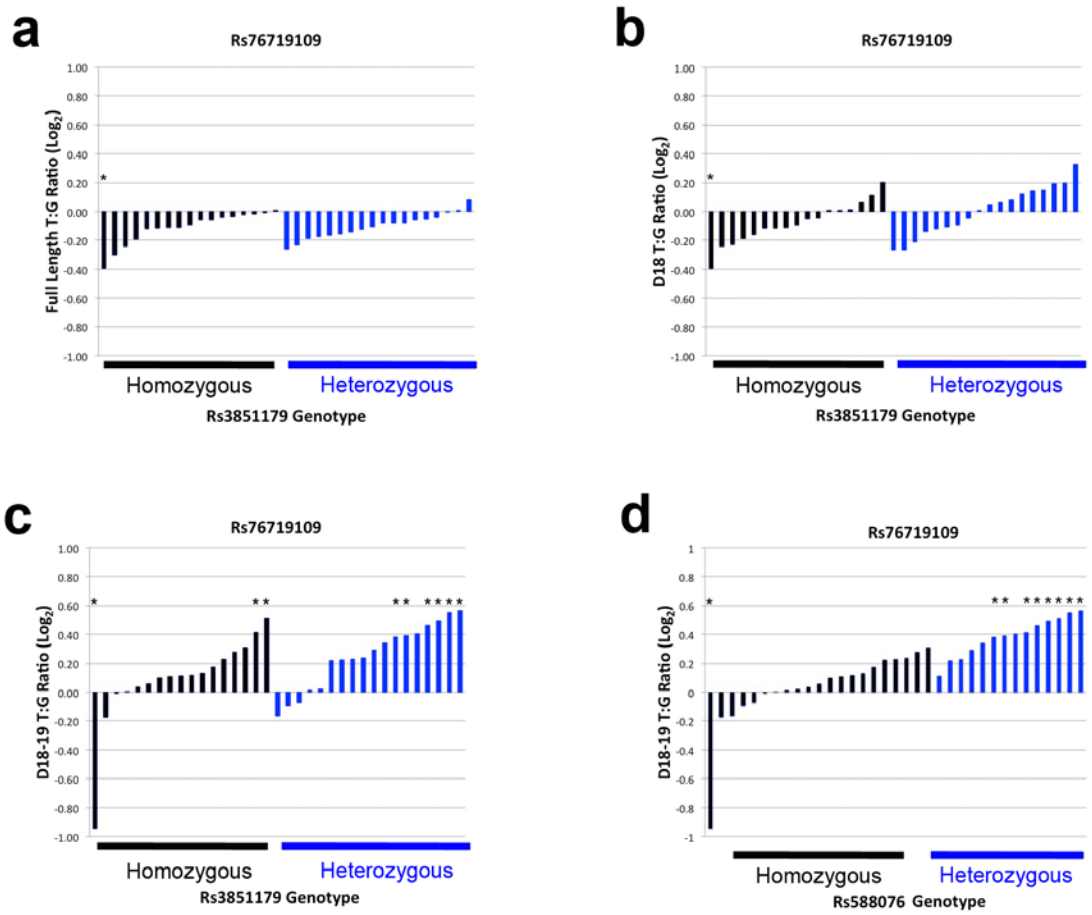

Figure 3.5 Evaluation of *PICALM* isoform AEI with respect to rs3851179.

The indicated *PICALM* isoforms were analyzed for AEI as a function of rs3851179 (a-c) or rs588076 (d). Each allelic ratio was normalized to the sample's gDNA ratio. a) The *full length PICALM* isoform contained exons 18-19 and showed equal allelic ratios, with a non-significant trend towards an increase in the G allele. b) *D18-PICALM* showed equal allelic ratios and c) *D18-19 PICALM* showed significant unequal allelic ratios in 9 samples (* $p<0.05$), d) The *D18-19 PICALM* AEI was associated with rs588076 heterozygosity. This pattern of significant AEI was not associated with sex, age or AD status ($p>0.05$).

Table 3.1 Rs76719019 Assay Non-AD Sample Demographics.

Sample ID	Age	Sex	PMI	MMSE	NIARI
C01	105	Male	3	24	No
C04	80	Male	3.5	28	No
C06	66	Female	4.5	30	No
C07	85	Male	2	30	Low likelihood
C08	84	Female	1.5	13	Intermediate likelihood
C09	79	Male	2.25	26	Low likelihood
C10	80	Male	3	27	No
C11	75	Female	3.5	29	No
C12	86	Female	2.25	30	Low likelihood
C13	95	Male	1.75	28	No
C17	72	Female	3.75	30	No
C18	91	Female	4	29	No
C19	86	Female	3.75	29	Low likelihood
C20	81	Male	2	30	Low likelihood
C22	82	Male	2.1	29	Low likelihood
C24	75	Male	4	28	High likelihood
C27	84	Female	2.5	30	Intermediate likelihood
C29	87	Female	2.41	28	Intermediate likelihood

Age, sex, PMI, MMSE and NIARI demographic of 18 non-AD samples in rs76719109 AEI assay.

Table 3.2 Rs76719019 Assay AD Sample Demographics.

Sample ID	Age	Sex	PMI	MMSE	NIARI
AD33	79	Female	3	11.5	High likelihood
AD37	83	Male	4	17.5	High likelihood
AD40	81	Male	3.5	17	High likelihood
AD42	86	Female	4.25	18	High likelihood
AD43	77	Male	3.5	19	High likelihood
AD44	84	Female	3.33	8	High likelihood
AD45	73	Male	2.75	N/A	N/A
AD46	81	Male	3.75	0	High likelihood
AD47	90	Female	2.8	4	High likelihood
AD48	78	Male	3.75	17.5	High likelihood
AD50	69	Male	4	4.5	Yes
AD51	75	Female	2.33	21.5	High likelihood
AD52	95	Male	4	7	High likelihood
AD54	84	Female	5	18	High likelihood
AD57	86	Female	3.25	7	High likelihood
AD59	78	Male	3.5	11	High likelihood
AD60	68	Female	3.25	26.5	High likelihood

Age, sex, PMI, MMSE and NIARI demographic of 17 AD samples in rs76719109 AEI assay.

Table 3.3 Rs592297 Assay Non-AD Sample Demographics.

Sample ID	Age	Sex	PMI	MMSE	NIARI
C01	105	Male	3	24	No
C02	92	Female	2.3	26	Low likelihood
C08	84	Female	1.5	13	Intermediate likelihood
C09	79	Male	2.25	26	Low likelihood
C10	80	Male	3	27	No
C11	75	Female	3.5	29	No
C13	95	Male	1.75	28	No
C15	77	Male	3.5	28	Low likelihood
C19	86	Female	3.75	29	Low likelihood
C20	81	Male	2	30	Low likelihood
C23	74	Male	4	26	No
C26	89	Female	1.75	30	Intermediate likelihood
C27	84	Female	2.5	30	Intermediate likelihood

Age, sex, PMI, MMSE and NIARI demographic of 13 non-AD samples in rs592297 AEI assay.

Table 3.4 Rs592297 Assay AD Sample Demographics.

Sample ID	Age	Sex	PMI	MMSE	NIARI
AD33	79	Female	3	11.5	High likelihood
AD43	77	Male	3.5	19	High likelihood
AD50	69	Male	4	4.5	Yes
AD51	75	Female	2.33	21.5	High likelihood
AD54	84	Female	5	18	High likelihood
AD58	90	Male	3.25	12	High likelihood

Age, sex, PMI, MMSE and NIARI demographic of 6 non-AD samples in rs592297 AEI assay.

Table 3.5 PCR Primers for Rs76719109 and Rs592297 AEI Assay.

SNP Assay	DNA	Primer Sense	Primer Sequence
rs76719109	cDNA	Sense	5'CCATCTCATCCCTGCGTGTCTCCGACTCAGxxxxxTGGAGTCAACCAGGTGAAAA
	cDNA	Anti-sense	5' CCTCTCTATGGGCAGTCGGTGATTTGGTTGCGTCATTACAGGA
	gDNA	Sense	5'CCATCTCATCCCTGCGTGTCTCCGACTCAGxxxxxTGGAGTCAACCAGGTGAAAA
	gDNA	Anti-sense	5' CCTCTCTATGGGCAGTCGGTGATAGGAGCTTTTTCAACTCACCA
rs592297	cDNA	Sense	5'CCATCTCATCCCTGCGTGTCTCCGACTCAGxxxxxTGAACACAGAAAAACTCCTAAAAA
	cDNA	Anti-sense	5' CCTCTCTATGGGCAGTCGGTGATGGCAGCATTTATTACCCCATT
	gDNA	Sense	5'CCATCTCATCCCTGCGTGTCTCCGACTCAGxxxxxTGAACACAGAAAAACTCCTAAAAA
	gDNA	Anti-sense	5' CCTCTCTATGGGCAGTCGGTGATTCTGTGAAAACTTGAGGTTAAAAA

"xxxxx" denotes 5 nucleic acid barcode, which is unique for each individual. Note that gDNA and cDNA were amplified by the same barcoded forward primers. Genomic DNA and cDNA were differentiated by the reverse primers.

Table 3.6 *PICALM* AEI Analysis of AD40 Shows Significant Unequal Rs76719109t To G Allele Ratios.

Rs76719109	Counts	Ratio (T/G)	mRNA ratio normalized to genomic ratio	P-value
Genomic **G** Allele	40357	1.01		0.89
Genomic **T** Allele	40880			
mRNA **G** Allele	88400	0.77	0.76	6.76×10^{-58}
mRNA **T** Allele	68141			
Isoforms				
D18 **G** Allele	17777	0.78	0.77	3.63×10^{-09}
D18 **T** Allele	13909			
D18-19 **G** Allele	4103	0.54	0.53	1.96×10^{-65}
D18-19 **T** Allele	2203			
Full length **G** Allele	66520	0.78	0.77	1.88×10^{-30}
Full length **T** Allele	52029			

Genomic DNA analysis shows an overall equal allelic representation while mRNA analysis shows significant AEI. This AEI was present in each of the three isoforms.

Table 3.7 *D18-19 PICALM* Shows Significant AEI in Nine Samples.

Sample	*D18-19* T:G Counts	Ratio (Normalized to genomic ratio)	P-Value
C01	2337:1793	1.30	8.66×10^{-3}
C11	13415:9508	1.47	7.91×10^{-34}
C20	745:523	1.43	2.78×10^{-3}
AD33	6136:4162	1.48	7.06×10^{-25}
AD43	1743:1321	1.31	9.47×10^{-3}
AD50	1529:1080	1.41	3.05×10^{-5}
AD51	5530:4243	1.33	5.27×10^{-5}
AD54	8893:6548	1.38	2.64×10^{-14}
AD40	2203:4103	0.53	1.96×10^{-65}

These *D18-19 PICALM* T:G allelic counts are the summation of three separate runs. AD samples are designated by an AD prefix while non-AD samples are designated with a C prefix.

Table 3.8 Samples with Robust AEI are Heterozygous for Three SNPs.

SNP	MAF in CEU	LD with rs3851179	LD with rs588076	LD with rs645299	LD with rs618629
rs588076	0.199	0.336	-	0.539	0.911
rs645299	0.306	0.665	0.539	-	0.525
rs618629	0.242	0.319	0.911	0.525	-

The samples C11 and AD33 were sequenced from exon 17 through exon 20. The samples were heterozygous for the indicated SNPs. These SNPs are in strong LD (Johnson et al., 2008) with each other and have similar frequencies for the minor allele (Sherry et al., 2001).

Table 3.9 Logistic Regression Modeling Of Rs3851179 and/or Rs588076 Effect(s) on AD.

Model	SNP	Odds Ratio	Confidence Interval	P value
rs588076	rs588076	0.8413	0.7151 - 0.9898	0.0372
rs3851179	rs3851179	0.7786	0.6819 - 0.8891	0.0002
rs3851179 + rs588076	rs3851179	0.7767	0.6604 - 0.9136	0.0023
rs3851179 + rs588076	rs588076	1.005	0.8238 - 1.227	0.959

In addition to the indicated SNPs, these models were adjusted for age of onset, APOE alleles, sex and contributing center.

Chapter 4
Discussion and Future Studies

Primary Findings

Recent AD GWAS have identified SNPs in several genes involved in receptor endocytosis. Several of these SNPs, including rs3851179, are near the gene phosphatidylinositol-binding clathrin assembly protein (*PICALM*) (Harold et al., 2009; Jun et al., 2010; Lambert et al., 2009; Pedraza et al., 2014; Seshadri et al., 2010). It is unclear how PICALM is involved in AD pathogenesis, thus a greater understanding of underlying molecular mechanisms of PICALM is needed. In this study I have characterized *PICALM* expression and splicing in human brain to help elucidate how this gene can be associated with AD.

The complexity of *PICALM* expression and splicing necessitated a complex analysis. PICALM is a ubiquitously expressed protein, which is highly expressed in brain tissue. Although PICALM is more prominent in microvessels, it is also present it neurons, astrocytes and oligodendrocytes (Baig et al., 2010; Bushlin et al., 2008; Parikh, Fardo, et al., 2014). *PICALM* mRNA expression is associated with AD risk SNP genotype, rs3851179, when cell type variation is included in the analysis. Furthermore, there are multiple splice variants present in the brain. Abundance of the splice variants expressed in brain was quantified by qPCR. The most abundant splice variant lacks exon 13, followed by exon 18-19, exon 2 and exon 2-4. It is critical to grasp an understanding of these splice variants as they will facilitate a better understanding of the molecular mechanisms influencing functionality of the protein.

An allelic expression imbalance (AEI) study was conducted to further study the association between rs3851179 and *PICALM*. Overall, the AD associated SNP rs3851179 does not demonstrate a detectable effect on global

PICALM AEI. However, a genetic variant, rs588076, subtly modulates a *PICALM* isoform lacking exons 18 and 19. Furthermore, an individual sample shows *PICALM* AEI. These results collectivity signify the intricacy of *PICALM* expression in the brain and thereby provide insights into current AD-related mechanisms studies, which have been largely conflicting and inconclusive.

Discussion and Future Directions

There are multiple implications of the presented findings. First, total mRNA *PICALM* expression was quantified using qPCR. Association of *PICALM* expression with rs3851179 was only seen when the statistical model was corrected with different cell type markers, i.e., neurons, astrocytes and microvessels, as covariates. The linear relationship between *PICALM* and different cell type markers is consistent with the immunohistochemical (IHC) results, where *PICALM* was present in microvessels and other cell types. The epitope for this particular antibody is the last 18 amino acids in the carboxyl-terminus of the protein, which is present in all isoforms of *PICALM*. Although several studies have tried to characterize and associate PICALM protein expression to AD phenotype in AD brains and AD animal models, only few studies have characterized mRNA expression (Allen et al., 2012; Baig et al., 2010; Karch et al., 2012; Parikh, Fardo, et al., 2014; Thomas et al., 2011). Allen et al, Baig et al and Karch et al did not detect an association between *PICALM* and AD, similar to our results. We analyzed the relationship between AD risk SNP, rs3851179, and mRNA expression. The rs3851179A allele is associated with increased mRNA expression; however, this expression may be modulated by the polymorphism in a cell-type specific manner because discerning the association between *PICALM* expression and rs3851179 was contingent upon including microvessel mRNA as a covariate within the regression model.

PICALM has been shown to be involved in intracellular trafficking, synaptic function and clathrin coated vesicle assembly (Harel et al., 2011; Harel, Wu, Mattson, Morris, & Yao, 2008). Currently, functional studies primarily focus on APP processing and subsequent toxic Aβ production to elucidate the role of PICALM expression in AD pathology (Kanatsu et al., 2014; Treusch et al., 2011; Xiao et al., 2012). Within the amyloidogenic pathway, APP is endocytosed from plasma membrane via CME and cleaved by secretase to produce toxic Aβ (Nordstedt, Caporaso, Thyberg, Gandy, & Greengard, 1993). The protective allele is associated with increased expression of the gene. Assuming mRNA expression is comparable to protein expression, increased expression of PICALM has been shown to influence the size and shape of the clathrin coated vesicle, as well as reduced function (Meyerholz et al., 2005; Tebar et al., 1999). Reduction in endocytosis of APP results in reduced Aβ release (Koo & Squazzo, 1994). In yeast and in rat neurons, PICALM has been shown to alter Aβ toxicity. Increasing PICALM decreased Aβ toxicity in a dose dependent manner (Treusch et al., 2011). Two other *in vitro* studies have shown opposite effect of increased PICALM, where increased PICALM expression, increased Aβ release as a result of increased APP endocytosis or increased gamma secretase endocytosis (Kanatsu et al., 2014; Xiao et al., 2012). However PICALM may not be the only culprit, AP180 is a homologue of PICALM and present exclusively in neurons. AP180 is also an accessory protein for CME and performs similar function. When PICALM and AP180 were decreased by RNAi by Wu et al. only AP180 knockdown affected Aβ generation (Wu, Matsuoka, Mattson, & Yao, 2009). PICALM and AP180 may compensate for one another in neurons or they may be dedicated to different processes in neurons (Bushlin et al., 2008; Wu et al., 2009; Wu, Mattson, & Yao, 2010).

PICALM is also present in microvessels, microglia and astrocytes (Ando et al., 2013; Karch et al., 2012; Parikh, Fardo, et al., 2014). The functional role of PICALM in these cell types is not well characterized. Our data show that *PICALM*

is highly expressed in microvessels and correlates positively with endothelial cell markers. This high localized expression suggests that PICALM actions in microvessels may be critical to PICALM actions in AD. One possible functional role for PICALM in microvessls Aβ clearance through the blood brain barrier. Theoretically, Lipoprotein Receptor-related Protein 1 (LRP1) can bind to Aβ in the brain and transport Aβ into the bloodstream by CME and exocytosis (Deane et al., 2004; Harasaki, Lubben, Harbour, Taylor, & Robinson, 2005). LRP1 can bind to Aβ indirectly thorough APOE (Bu, 2009). In one GWAS, *PICALM* showed significant reduced risk for AD when corrected for APOE4 genotype, suggesting a link between APOE and *PICALM* (Jun et al., 2010; Sweet et al., 2012). Increased *PICALM* expression, may increase CME of APOE-Aβ complex bound to LRP1, promoting clearance of Aβ. An association between CSF Aβ42 level and *PICALM* AD risk SNP, further support this hypothesis (Schjeide et al., 2011). However, APOE and CSF Aβ42 level did not associate with rs3851179 in replication study and further meta-analyzes study (Kauwe et al., 2011; Naj et al., 2011).

Implications of splice variants on function

I have identified over 20 different splice variants for *PICALM*. The role of PICALM protein encoded by these variants has not been thoroughly researched. Several isoforms lack key domains and protein binding motifs needed for proper function. There are three sites important for AP_2 binding. Meyerholz et al. have described the importance of these sites and their effect on PICALM function in clathrin cage formation and size. The most abundant *PICALM* isoform lacks exon 13, which encodes a DPF binding motif that binds to AP_2 (Meyerholz et al., 2005). Similarly, some isoforms lack exons 18-19 which encode a protein domain that is important for clathrin binding (Scotland et al., 2012). Lastly, isoforms that lack exon 2 have a premature stop codon and encode a truncated PICALM fragment (Figure 1.2). There are multiple adaptor and accessory proteins involved in CME which may enable PICALM to be still functional in different

processes, such as cell proliferation, endosome transport, and vesicle transport (Dreyling et al., 1996; Meyerholz et al., 2005; Scotland et al., 2012; Tebar et al., 1999). Different isoforms could be important for different processes. PICALM bound to AP_2 has been shown to be involved in degradation of the APP carboxyl-terminus fragment, isoforms lacking exon 13 and/or 14 could influence this process since isoforms lacking these exons would encode a protein with reduced AP_2 binding capability; whereas isoforms lacking exons 18-19 could reduced endocytosis of APP from plasma membrane since isoforms lacking exons 18-19 would have reduced clathrin binding and subsequently reduced CME (Tian, Chang, Fan, Flajolet, & Greengard, 2013; Xiao et al., 2012). Endocytosis studies with protein encoded with these *PICALM* variants isoforms could lead to a better understanding of the criticality of these variants.

PICALM isoforms can be cell type specific or the level of expression may be cell type specific. Our results show that D13, D18-19, and D2 isoforms correlate positively with microvessel mRNA and GFAP, but negatively with SYN; whereas the D2-4 isoform correlates positively with neuronal marker SYN (Table 2.2) This means exons 2-4 could be preferentially spliced by neurons to produce D2-4. Although D2-4 is a rare isoform, it produces a truncated protein that would be non-functional. When Ando et al. used three different antibodies to stain PICALM in human brain tissue, the antibody binding the epitopes encoded within exon 10, exon 13, and last 18 amino acids of the carboxyl-terminus had different immunoreactivity between the three antibodies (Ando et al., 2013). Our results indicate that HPA019053 antibody should label stronger in neurons that the other two antibodies. The expression and function of these isoforms in specific cell types warrant more investigation.

Genetic association with splice variants

The relationship between the primary AD-associated SNP and the SNPs that are associated with *PICALM* splice variants requires further clarification. The primary *PICALM* AD risk SNP is rs3851179. However two other genetic variations have associated with *PICALM* isoforms. The first of these SNPs is rs592297, which associated with *D2-4 PICALM* isoform in our linear regression analysis. Rs592297 is a synonymous SNP located within exon 5 and has been predicted to be an exon splicing enhancer (Harold et al., 2009; Schnetz-Boutaud et al., 2012). Further experimentation is needed to elucidate if rs592297 is a functional SNP influencing exon2-4 splicing. If rs592297 is a functional SNP, the protein encoded by *D2-4 PICALM* is incomplete and most likely non-functional. This is a rare isoform and the SNP was not robustly associated with AD in GWAS (Harold et al., 2009). The impact of this SNP may be low but it could contribute to AD risk is a cumulative fashion with rs3851179.

The second SNP that was associated with a *PICALM* isoform was rs588076, which was associated with the *D18-19 PICALM* isoform. Rs588076 is an intronic SNP located within intron 17. Rs588076 may be the functional SNP or may be in high LD with the functional SNP to influence splicing of D18-19 isoform. Eight out of fourteen individuals, heterozygous for rs588076, showed significant AEI for *D18-19 PICALM.* A replicate study with more individuals would be beneficial. The SNP itself may not be the functional SNP, rather it may work synergistically with another SNP to influence splicing of exons 18 and 19 or it may be in high LD with the functional SNP. There were other SNPs within the latter part of the gene that were heterozygous in individuals showing high AEI. Most of the SNPs were in high LD with each other, thus multiple SNPs could be influencing the splicing of exons 18-19 synergistically. Overall, the effect of rs588076 on *D18-19 PICALM* should be further studied to elucidate if rs588076 is the functional SNP, or another SNP in high LD with rs588076 is the culprit, as it may have functional implications beyond AD.

Isoforms lacking exons 18-19 encode PICALM that lacks a part of the clathrin binding domain of *PICALM*. How the loss of exons 18-19 translates to PICALM function should be further examined. Interestingly, rs588076C allele has been associated with systolic blood pressure response to calcium channel blocking drug in hypertensive patients (Kamide et al., 2013). There is ambiguouity about how *PICALM* SNP can be involved in pressure response, calcium channel regulation or calcium uptake. To gain greater insight, mRNA expression of total *PICALM* and *D18-19 PICALM* should be quantified in vascular and heart tissue. When we quantified the isoform in brain tissue it was 1-2% of total *PICALM* expression. However this isoform may be expressed more in other tissues. Furthermore, function of the encoded *D18-19 PICALM* protein should be studied relative to vascular smooth muscle cells and factors that influence vasodilation of arteries.

Analysis of SNP effect

Two primary methods were used to analyze the genetic effect of the AD risk SNP rs3851179 on gene expression. First, real time quantitative PCR (qPCR) was used to quantify mRNA expression of total PICALM and several splice variants, and then statistically analyzed for an association with AD, rs3851179, and brain specific cell types. Second, next generation sequencing was used to measure the incidence of SNP alleles to see if alleles are unequally represented, i.e., whether one allele is associated with higher expression of the gene. Both methods have their strengths and weaknesses. Selected aspects will be discussed more thoroughly below. In brief, the strengths of the qPCR assay include: the ability to analyze SNPs in intronic and non-coding region, quantifying the gene expression with respect to control genes and standard curve, and sensitive analysis of low expression genes. Conversely, the weaknesses of qPCR include: inter-individual variability can confound analysis and the ability to quantify only one isoform in an assay. Whereas, the AEI study assay can detect

multiple isoforms and avoids inter-individual variability by comparing with a person. However, the weaknesses of AEI studies includes that the assay requires that the genes have a higher expression, a common SNP in the coding region of the gene that is detectable with an amplicon of the appropriate size for sequencing.

Intronic or noncoding SNPs can be indirectly studied using the AEI method by using marker SNPs within the gene that are in high LD with the SNP of interest. Whereas in the qPCR method, any SNP, coding and noncoding, can be genotyped and can be analyzed for an association directly. We genotyped rs3851179 in our sample set, and quantified PICALM using qPCR for the association. Whereas, for the AEI study we used two exonic SNP rs76719109 and rs592297 as marker SNPs and then further analyzed the data for the AD associated SNP. To analyze SNP effect on gene expression, AEI assays require exonic SNPs that are sufficiently abundant to ensure numbers of samples that are well powered for analysis.

Another advantage of qPCR is the sensitive quantification of copy numbers, whereas in AEI the gene expression is not quantified, rather it is the relative comparison of transcript or allele present within the sample. With qPCR, expression of *PICALM* can be compared among isoforms of *PICALM* as well as other genes in the brain; which was especially beneficial to us since our results showed a cell type effect. We could only compare *PICALM* expression to SYN, GFAP and microvessel mRNA using the qPCR method. A common concern with PCR-based assays is PCR bias. However in both our qPCR and AEI studies, we included standard curves which were linear and hence PCR bias does appear to be an issue in our studies. In particular however, we note that we did not compare the relative abundance of one transcript to another transcript in the AEI studies because of concerns regarding PCR bias between isoforms in this assay.

AEI is useful for initial assessment of allele expression, however for more multidimensional assessment, qPCR analysis is necessary.

Another consideration is amplicon size limitations which are present in both methods. Although next generation sequencing methods have advanced in amplicon length reads, at the time our study the average length read was around 150-200 bp by Ion Torrent. In qPCR, the amplicons must be less than 200 bp to ensure high efficiency amplification. Using qPCR, only one isoform can be analyzed at a time. Whereas, with the AEI approach, we were able to analyzed three different isoforms in one study. Overall, experimental design was a challenge for qPCR and AEI, as there were multiple exons that were alternatively spliced.

In our results, we see an association of rs3851179 on total *PICALM* expression using qPCR, however we do not see equal allelic representation in the AEI study. These results have two interpretations. First, the qPCR assay relies upon normalizing the mRNA copy numbers for housekeeping genes, and cell type specific markers. For ubiquitously expressed genes, this normalization can be beneficial in discriminating cell specific effects. qPCR analyses are advantageous in discerning gene effect on expression of a gene present in multiple cells. PICALM is expressed in endothelial cells, microglia, astrocytes and neurons. The effect of the SNP on gene expression could be more in one type than other due to differences in transcription or splicing factors. Normalizing to these cell types could help discover an association. In AEI study, samples are normalized to the genomic allelic ratio and there is no cell type or housekeeping gene normalization. As an example, consider the possibility that *PICALM* is highly expressed in microvessels where there is no SNP effect, compared to expression in neurons where there is a SNP effect but there is low copy number of the gene. The SNP effect will be masked by the allelic representation of microvessel cells mRNA content, because all cells are homogenized in the sample. The second of the different results obtained with the qPCR and AEI

studies was that the association of *PICALM* expression with rs3851179 by qPCR relies upon statistical association. The statistical association could be due to an unknown confounding factor such that the linear regression analysis of qPCR results is a statistical artifact.

PICALM in human disease

PICALM has been implicated in two human diseases, acute leukemia and AD. PICALM was first isolated from the U937 cell line used to study acute leukemia. Chromosomal translocation of t(10;11)(p13;q14) results in *AF10/CALM* or *CALM/AF10* fusion gene and is associated with poor prognosis (Ben Abdelali et al., 2013; Dreyling et al., 1996). The role of the fusion protein in leukemia is still being elucidated. There are multiple splice variants present for both genes. In the PICALM/AF10 chromosomal translocation, the chromosome breakpoint occurs in the latter part of *PICALM*, usually around intron 17-19 with the resulting mRNA encoding in frame and out of frame transcripts (Silliman et al., 1998). (Caudell & Aplan, 2008). Although the fusion transcript is rare, the effect of rs588076 on exon 18-19 splicing may be critical for the translated leukemogenic protein.

PICALM is one of the few genes associated with AD through GWAS. AD is a complex disease with complex genetic penetrance. *PICALM* locus has been consistently associated with AD, however, there has been debate if *PICALM* SNPs are protective in all populations and/or if rs3851179 is the primary AD associated SNP for the gene (Harold et al., 2009; Naj et al., 2011; W. Xu, Tan, & Yu, 2014). It is unclear how the SNP maybe be contributing to the GWAS outcome. A number of studies have expounded the role of the PICALM protein in AD pathological pathway. However, few studies have tried to elucidate the function of the AD SNP genotype in regulating expression and splicing of *PICALM*. The SNP itself is ~80,000 bp from the coding region of the gene,

suggesting that this SNP may be in LD with the functional SNP within the gene, in the *PICALM* promoter region, and/or located on a distant-acting transcriptional regulatory element.

To understand the effect of the SNP on AD, the effects of the AD associated SNP on *PICALM* mRNA must be elucidated. The rs3851179A minor allele is protective for AD risk. Our qPCR results show that presence of A allele is associated with increased *total PICALM* and *D13-PICALM* expression. I interpret these results as having two possible meanings. The first interpretation focuses on total *PICALM*. An increase in *total PICALM* expression results in increased PICALM expression, which disrupts CME by altering clathrin coated vesicle size and shape. This, in turn, reduces endocytosis of proteins like transferrin. In contrast, increased PICALM has ben shown to increase encocytosis of proteins like APP, leading to increased Aβ production (Tebar et al., 1999; Xiao et al., 2012). Thus, increased PICALM could result in a loss of function, as shown by Tebar et al., because disruption of CME reduces transferrin endocytosis. However, increased PICALM could be a gain of function resulting in increased Aβ. The effect of PICALM may be in modulating in a ligand specific manner. The second interpretation of the SNP association focuses upon increased *D13-PICALM* expression. This would result in increased PICALM protein that has reduced functional capability and thus decreased CME. Hence, the protein encoded by isoforms lacking exon 13 needs to further studied within the AD pathway. Overall, there is still debate whether overexpression of PICALM exacerbates or rescues AD phenotypes or pathology. Further studies with different protein isoforms could elucidate PICALM function in AD.

One would hope that understanding how rs3851179 modulates *PICALM* expression and splicing to influence AD risk may allow us to develop novel therapeutics that mimic the protective effects of this SNP, and thereby reduce AD

risk. However this will be challenging because PICALM is ubiquitously expressed and endocytosis is a critical process for many physiological processes. Furthermore, alterations in PICALM expression have varied results on clathrin coated vesicle size and shape and CME (Meyerholz et al., 2005; Tebar et al., 1999). Up regulating or down regulating PICALM might require a fine balance rather than sheer expression changeability. Evaluating actions of AD associated SNP on *PICALM* expression and subsequent protein expression will determine the effects of encoded isoforms on CME and thereby provide insights into AD-related mechanisms.

References

Allen, M., Zou, F., Chai, H. S., Younkin, C. S., Crook, J., Pankratz, V. S., . . . Ertekin-Taner, N. (2012). Novel late-onset Alzheimer disease loci variants associate with brain gene expression. *Neurology, 79*(3), 221-228. doi: 10.1212/WNL.0b013e3182605801

Ando, K., Brion, J. P., Stygelbout, V., Suain, V., Authelet, M., Dedecker, R., . . . Duyckaerts, C. (2013). Clathrin adaptor CALM/PICALM is associated with neurofibrillary tangles and is cleaved in Alzheimer's brains. *Acta Neuropathol, 125*(6), 861-878. doi: 10.1007/s00401-013-1111-z

Avramopoulos, D. (2009). Genetics of Alzheimer's disease: recent advances. *Genome Med, 1*(3), 34. doi: 10.1186/gm34

Baig, S., Joseph, S. A., Tayler, H., Abraham, R., Owen, M. J., Williams, J., . . . Love, S. (2010). Distribution and expression of picalm in Alzheimer disease. *J Neuropathol Exp Neurol, 69*(10), 1071-1077. doi: 10.1097/NEN.0b013e3181f52e01

Bali, J., Halima, S. B., Felmy, B., Goodger, Z., Zurbriggen, S., & Rajendran, L. (2010). Cellular basis of Alzheimer's disease. *Ann Indian Acad Neurol, 13*(Suppl 2), S89-93. doi: 10.4103/0972-2327.74251

Ben Abdelali, R., Asnafi, V., Petit, A., Micol, J. B., Callens, C., Villarese, P., . . . Macintyre, E. (2013). The prognosis of CALM-AF10-positive adult T-cell acute lymphoblastic leukemias depends on the stage of maturation arrest. *Haematologica, 98*(11), 1711-1717. doi: 10.3324/haematol.2013.086082

Bertram, L., McQueen, M. B., Mullin, K., Blacker, D., & Tanzi, R. E. (2007). Systematic meta-analyses of Alzheimer disease genetic association studies: the AlzGene database. *Nat Genet, 39*(1), 17-23. doi: 10.1038/ng1934

Blennow, K., & Hampel, H. (2003). CSF markers for incipient Alzheimer's disease. *Lancet Neurol, 2*(10), 605-613.

Braak, H., & Braak, E. (1991). Neuropathological stageing of Alzheimer-related changes. *Acta Neuropathol, 82*(4), 239-259.

Bu, G. (2009). Apolipoprotein E and its receptors in Alzheimer's disease: pathways, pathogenesis and therapy. *Nat Rev Neurosci, 10*(5), 333-344. doi: 10.1038/nrn2620

Burdick, D., Soreghan, B., Kwon, M., Kosmoski, J., Knauer, M., Henschen, A., . . . Glabe, C. (1992). Assembly and aggregation properties of synthetic Alzheimer's A4/beta amyloid peptide analogs. *J Biol Chem, 267*(1), 546-554.

Bushlin, I., Petralia, R. S., Wu, F., Harel, A., Mughal, M. R., Mattson, M. P., & Yao, P. J. (2008). Clathrin assembly protein AP180 and CALM differentially control axogenesis and dendrite outgrowth in embryonic hippocampal neurons. *J Neurosci, 28*(41), 10257-10271. doi: 10.1523/JNEUROSCI.2471-08.2008

Caudell, D., & Aplan, P. D. (2008). The role of CALM-AF10 gene fusion in acute leukemia. *Leukemia, 22*(4), 678-685. doi: 10.1038/sj.leu.2405074

Chen, L. H., Kao, P. Y., Fan, Y. H., Ho, D. T., Chan, C. S., Yik, P. Y., . . . Song, Y. Q. (2012). Polymorphisms of CR1, CLU and PICALM confer

susceptibility of Alzheimer's disease in a southern Chinese population. *Neurobiol Aging, 33*(1), 210 e211-217. doi: 10.1016/j.neurobiolaging.2011.09.016

Chomczynski, P., & Sacchi, N. (1987). Single-step method of RNA isolation by acid guanidinium thiocyanate-phenol-chloroform extraction. *Anal Biochem, 162*(1), 156-159. doi: 10.1006/abio.1987.9999

Corneveaux, J. J., Myers, A. J., Allen, A. N., Pruzin, J. J., Ramirez, M., Engel, A., . . . Huentelman, M. J. (2010). Association of CR1, CLU and PICALM with Alzheimer's disease in a cohort of clinically characterized and neuropathologically verified individuals. *Hum Mol Genet, 19*(16), 3295-3301. doi: 10.1093/hmg/ddq221

Cruts, M., Theuns, J., & Van Broeckhoven, C. (2012). Locus-specific mutation databases for neurodegenerative brain diseases. *Hum Mutat, 33*(9), 1340-1344. doi: 10.1002/humu.22117

D'Angelo, F., Vignaud, H., Di Martino, J., Salin, B., Devin, A., Cullin, C., & Marchal, C. (2013). A yeast model for amyloid-beta aggregation exemplifies the role of membrane trafficking and PICALM in cytotoxicity. *Dis Model Mech, 6*(1), 206-216. doi: 10.1242/dmm.010108

Deane, R., Wu, Z., Sagare, A., Davis, J., Du Yan, S., Hamm, K., . . . Zlokovic, B. V. (2004). LRP/amyloid beta-peptide interaction mediates differential brain efflux of Abeta isoforms. *Neuron, 43*(3), 333-344. doi: 10.1016/j.neuron.2004.07.017

Deshpande, A., Mina, E., Glabe, C., & Busciglio, J. (2006). Different conformations of amyloid beta induce neurotoxicity by distinct mechanisms in human cortical neurons. *J Neurosci, 26*(22), 6011-6018. doi: 10.1523/JNEUROSCI.1189-06.2006

Dreyling, M. H., Martinez-Climent, J. A., Zheng, M., Mao, J., Rowley, J. D., & Bohlander, S. K. (1996). The t(10;11)(p13;q14) in the U937 cell line results in the fusion of the AF10 gene and CALM, encoding a new member of the AP-3 clathrin assembly protein family. *Proc Natl Acad Sci U S A, 93*(10), 4804-4809.

Eisenstein, M. (2011). Genetics: finding risk factors. *Nature, 475*(7355), S20-22. doi: 10.1038/475S20a

Exome Variant Server. Retrieved September 1, 2013, from http://evsgswashingtonedu/EVS/

Fargo, K., & Bleiler, L. (2014). Alzheimer's Association report. *Alzheimers Dement, 10*(2), e47-92.

Feinkohl, I., Keller, M., Robertson, C. M., Morling, J. R., Williamson, R. M., Nee, L. D., . . . Edinburgh Type 2 Diabetes Study, I. (2013). Clinical and subclinical macrovascular disease as predictors of cognitive decline in older patients with type 2 diabetes: the Edinburgh Type 2 Diabetes Study. *Diabetes Care, 36*(9), 2779-2786. doi: 10.2337/dc12-2241

Fleige, S., & Pfaffl, M. W. (2006). RNA integrity and the effect on the real-time qRT-PCR performance. *Mol Aspects Med, 27*(2-3), 126-139. doi: 10.1016/j.mam.2005.12.003

Flicek, P., Amode, M. R., Barrell, D., Beal, K., Billis, K., Brent, S., . . . Searle, S. M. (2014). Ensembl 2014. *Nucleic Acids Res, 42*(Database issue), D749-755. doi: 10.1093/nar/gkt1196

Folstein, M. F., Folstein, S. E., & McHugh, P. R. (1975). "Mini-mental state". A practical method for grading the cognitive state of patients for the clinician. *J Psychiatr Res, 12*(3), 189-198.

Gamblin, T. C., Chen, F., Zambrano, A., Abraha, A., Lagalwar, S., Guillozet, A. L., . . . Cryns, V. L. (2003). Caspase cleavage of tau: linking amyloid and neurofibrillary tangles in Alzheimer's disease. *Proc Natl Acad Sci U S A, 100*(17), 10032-10037. doi: 10.1073/pnas.1630428100

Gatz, M., Reynolds, C. A., Fratiglioni, L., Johansson, B., Mortimer, J. A., Berg, S., . . . Pedersen, N. L. (2006). Role of genes and environments for explaining Alzheimer disease. *Arch Gen Psychiatry, 63*(2), 168-174. doi: 10.1001/archpsyc.63.2.168

Glenner, G. G., & Wong, C. W. (1984). Alzheimer's disease: initial report of the purification and characterization of a novel cerebrovascular amyloid protein. *Biochem Biophys Res Commun, 120*(3), 885-890.

Goate, A., Chartier-Harlin, M. C., Mullan, M., Brown, J., Crawford, F., Fidani, L., . . . et al. (1991). Segregation of a missense mutation in the amyloid precursor protein gene with familial Alzheimer's disease. *Nature, 349*(6311), 704-706. doi: 10.1038/349704a0

Grant, B. D. a. S., M. Intracellular trafficking (January 21, 2006), WormBook, ed. The C. elegans Research Community, WormBook, doi/10.1895/wormbook.1.77.1,http://www.wormbook.org.

Grundke-Iqbal, I., Iqbal, K., Tung, Y. C., Quinlan, M., Wisniewski, H. M., & Binder, L. I. (1986). Abnormal phosphorylation of the microtubule-associated protein tau (tau) in Alzheimer cytoskeletal pathology. *Proc Natl Acad Sci U S A, 83*(13), 4913-4917.

Hanger, D. P., Byers, H. L., Wray, S., Leung, K. Y., Saxton, M. J., Seereeram, A., . . . Anderton, B. H. (2007). Novel phosphorylation sites in tau from Alzheimer brain support a role for casein kinase 1 in disease pathogenesis. *J Biol Chem, 282*(32), 23645-23654. doi: 10.1074/jbc.M703269200

Harasaki, K., Lubben, N. B., Harbour, M., Taylor, M. J., & Robinson, M. S. (2005). Sorting of major cargo glycoproteins into clathrin-coated vesicles. *Traffic, 6*(11), 1014-1026. doi: 10.1111/j.1600-0854.2005.00341.x

Harel, A., Mattson, M. P., & Yao, P. J. (2011). CALM, a clathrin assembly protein, influences cell surface GluR2 abundance. *Neuromolecular Med, 13*(1), 88-90. doi: 10.1007/s12017-010-8142-6

Harel, A., Wu, F., Mattson, M. P., Morris, C. M., & Yao, P. J. (2008). Evidence for CALM in directing VAMP2 trafficking. *Traffic, 9*(3), 417-429. doi: 10.1111/j.1600-0854.2007.00694.x

Harold, D., Abraham, R., Hollingworth, P., Sims, R., Gerrish, A., Hamshere, M. L., . . . Williams, J. (2009). Genome-wide association study identifies variants at CLU and PICALM associated with Alzheimer's disease. *Nat Genet, 41*(10), 1088-1093. doi: 10.1038/ng.440

Hollingworth, P., Harold, D., Sims, R., Gerrish, A., Lambert, J. C., Carrasquillo, M. M., . . . Williams, J. (2011). Common variants at ABCA7, MS4A6A/MS4A4E, EPHA1, CD33 and CD2AP are associated with Alzheimer's disease. *Nat Genet, 43*(5), 429-435. doi: 10.1038/ng.803

Huang, F., Khvorova, A., Marshall, W., & Sorkin, A. (2004). Analysis of clathrin-mediated endocytosis of epidermal growth factor receptor by RNA interference. *J Biol Chem, 279*(16), 16657-16661. doi: 10.1074/jbc.C400046200

Hyman, B. T., & Trojanowski, J. Q. (1997). Consensus recommendations for the postmortem diagnosis of Alzheimer disease from the National Institute on Aging and the Reagan Institute Working Group on diagnostic criteria for the neuropathological assessment of Alzheimer disease. *J Neuropathol Exp Neurol, 56*(10), 1095-1097.

Jackson, D. E. (2003). The unfolding tale of PECAM-1. *FEBS Lett, 540*(1-3), 7-14.

Jentarra, G. M., Rice, S. G., Olfers, S., Saffen, D., & Narayanan, V. (2011). Evidence for population variation in TSC1 and TSC2 gene expression. *BMC Med Genet, 12*, 29. doi: 10.1186/1471-2350-12-29

Jiang, H., & Wong, W. H. (2009). Statistical inferences for isoform expression in RNA-Seq. *Bioinformatics, 25*(8), 1026-1032. doi: 10.1093/bioinformatics/btp113

Jiang, T., Yu, J. T., Tan, M. S., Wang, H. F., Wang, Y. L., Zhu, X. C., . . . Tan, L. (2014). Genetic variation in PICALM and Alzheimer's disease risk in Han Chinese. *Neurobiol Aging, 35*(4), 934 e931-933. doi: 10.1016/j.neurobiolaging.2013.09.014

Johnson, A. D., Handsaker, R. E., Pulit, S. L., Nizzari, M. M., O'Donnell, C. J., & de Bakker, P. I. (2008). SNAP: a web-based tool for identification and annotation of proxy SNPs using HapMap. *Bioinformatics, 24*(24), 2938-2939. doi: 10.1093/bioinformatics/btn564

Jones, B. L., & Swallow, D. M. (2011). The impact of cis-acting polymorphisms on the human phenotype. *Hugo J, 5*(1-4), 13-23. doi: 10.1007/s11568-011-9155-4

Jun, G., Naj, A. C., Beecham, G. W., Wang, L. S., Buros, J., Gallins, P. J., . . . Schellenberg, G. D. (2010). Meta-analysis confirms CR1, CLU, and PICALM as alzheimer disease risk loci and reveals interactions with APOE genotypes. *Arch Neurol, 67*(12), 1473-1484. doi: 10.1001/archneurol.2010.201

Kamide, K., Asayama, K., Katsuya, T., Ohkubo, T., Hirose, T., Inoue, R., . . . Imai, Y. (2013). Genome-wide response to antihypertensive medication using home blood pressure measurements: a pilot study nested within the HOMED-BP study. *Pharmacogenomics, 14*(14), 1709-1721. doi: 10.2217/pgs.13.161

Kanatsu, K., Morohashi, Y., Suzuki, M., Kuroda, H., Watanabe, T., Tomita, T., & Iwatsubo, T. (2014). Decreased CALM expression reduces Abeta42 to total Abeta ratio through clathrin-mediated endocytosis of gamma-secretase. *Nat Commun, 5*, 3386. doi: 10.1038/ncomms4386

Kang, J., Lemaire, H. G., Unterbeck, A., Salbaum, J. M., Masters, C. L., Grzeschik, K. H., . . . Muller-Hill, B. (1987). The precursor of Alzheimer's disease amyloid A4 protein resembles a cell-surface receptor. *Nature, 325*(6106), 733-736. doi: 10.1038/325733a0

Karch, C. M., Jeng, A. T., Nowotny, P., Cady, J., Cruchaga, C., & Goate, A. M. (2012). Expression of novel Alzheimer's disease risk genes in control and Alzheimer's disease brains. *PLoS One, 7*(11), e50976. doi: 10.1371/journal.pone.0050976

Kauwe, J. S., Cruchaga, C., Karch, C. M., Sadler, B., Lee, M., Mayo, K., . . . Goate, A. M. (2011). Fine mapping of genetic variants in BIN1, CLU, CR1 and PICALM for association with cerebrospinal fluid biomarkers for Alzheimer's disease. *PLoS One, 6*(2), e15918. doi: 10.1371/journal.pone.0015918

Klunk, W. E., Engler, H., Nordberg, A., Wang, Y., Blomqvist, G., Holt, D. P., . . . Langstrom, B. (2004). Imaging brain amyloid in Alzheimer's disease with Pittsburgh Compound-B. *Ann Neurol, 55*(3), 306-319. doi: 10.1002/ana.20009

Koo, E. H., & Squazzo, S. L. (1994). Evidence that production and release of amyloid beta-protein involves the endocytic pathway. *J Biol Chem, 269*(26), 17386-17389.

Lambert, J. C., Heath, S., Even, G., Campion, D., Sleegers, K., Hiltunen, M., . . . Amouyel, P. (2009). Genome-wide association study identifies variants at CLU and CR1 associated with Alzheimer's disease. *Nat Genet, 41*(10), 1094-1099. doi: 10.1038/ng.439

Lambert, J. C., Ibrahim-Verbaas, C. A., Harold, D., Naj, A. C., Sims, R., Bellenguez, C., . . . Amouyel, P. (2013). Meta-analysis of 74,046 individuals identifies 11 new susceptibility loci for Alzheimer's disease. *Nat Genet, 45*(12), 1452-1458. doi: 10.1038/ng.2802

Lambert, J. C., Zelenika, D., Hiltunen, M., Chouraki, V., Combarros, O., Bullido, M. J., . . . Amouyel, P. (2011). Evidence of the association of BIN1 and PICALM with the AD risk in contrasting European populations. *Neurobiol Aging, 32*(4), 756 e711-755. doi: 10.1016/j.neurobiolaging.2010.11.022

Lee, J. H., Cheng, R., Barral, S., Reitz, C., Medrano, M., Lantigua, R., . . . Mayeux, R. (2011). Identification of novel loci for Alzheimer disease and replication of CLU, PICALM, and BIN1 in Caribbean Hispanic individuals. *Arch Neurol, 68*(3), 320-328. doi: 10.1001/archneurol.2010.292

Li, H. L., Shi, S. S., Guo, Q. H., Ni, W., Dong, Y., Liu, Y., . . . Wu, Z. Y. (2011). PICALM and CR1 variants are not associated with sporadic Alzheimer's disease in Chinese patients. *J Alzheimers Dis, 25*(1), 111-117. doi: 10.3233/JAD-2011-101917

Ling, I. F., Bhongsatiern, J., Simpson, J. F., Fardo, D. W., & Estus, S. (2012). Genetics of clusterin isoform expression and Alzheimer's disease risk. *PLoS One, 7*(4), e33923. doi: 10.1371/journal.pone.0033923

Liu, C. C., Kanekiyo, T., Xu, H., & Bu, G. (2013). Apolipoprotein E and Alzheimer disease: risk, mechanisms and therapy. *Nat Rev Neurol, 9*(2), 106-118. doi: 10.1038/nrneurol.2012.263

Liu, G., Zhang, S., Cai, Z., Ma, G., Zhang, L., Jiang, Y., . . . Li, K. (2013). PICALM gene rs3851179 polymorphism contributes to Alzheimer's disease in an Asian population. *Neuromolecular Med, 15*(2), 384-388. doi: 10.1007/s12017-013-8225-2

Malik, M., Simpson, J. F., Parikh, I., Wilfred, B. R., Fardo, D. W., Nelson, P. T., & Estus, S. (2013). CD33 Alzheimer's Risk-Altering Polymorphism, CD33 Expression, and Exon 2 Splicing. *J Neurosci, 33*(33), 13320-13325. doi: 10.1523/JNEUROSCI.1224-13.2013

Maurer, K., Volk, S., & Gerbaldo, H. (1997). Auguste D and Alzheimer's disease. *Lancet, 349*(9064), 1546-1549. doi: 10.1016/S0140-6736(96)10203-8

Meyerholz, A., Hinrichsen, L., Groos, S., Esk, P. C., Brandes, G., & Ungewickell, E. J. (2005). Effect of clathrin assembly lymphoid myeloid leukemia protein depletion on clathrin coat formation. *Traffic, 6*(12), 1225-1234. doi: 10.1111/j.1600-0854.2005.00355.x

Mirra, S. S., Heyman, A., McKeel, D., Sumi, S. M., Crain, B. J., Brownlee, L. M., . . . Berg, L. (1991). The Consortium to Establish a Registry for Alzheimer's Disease (CERAD). Part II. Standardization of the neuropathologic assessment of Alzheimer's disease. *Neurology, 41*(4), 479-486.

Miyashita, A., Koike, A., Jun, G., Wang, L. S., Takahashi, S., Matsubara, E., . . . Kuwano, R. (2013). SORL1 is genetically associated with late-onset Alzheimer's disease in Japanese, Koreans and Caucasians. *PLoS One, 8*(4), e58618. doi: 10.1371/journal.pone.0058618

Mondal, A. K., Sharma, N. K., Elbein, S. C., & Das, S. K. (2013). Allelic expression imbalance screening of genes in chromosome 1q21-24 region to identify functional variants for Type 2 diabetes susceptibility. *Physiol Genomics, 45*(13), 509-520. doi: 10.1152/physiolgenomics.00048.2013

Morgan, K. (2011). The three new pathways leading to Alzheimer's disease. *Neuropathology and applied neurobiology, 37*(4), 353-357. doi: 10.1111/j.1365-2990.2011.01181.x

Mudher, A., Shepherd, D., Newman, T. A., Mildren, P., Jukes, J. P., Squire, A., . . . Lovestone, S. (2004). GSK-3beta inhibition reverses axonal transport defects and behavioural phenotypes in Drosophila. *Mol Psychiatry, 9*(5), 522-530. doi: 10.1038/sj.mp.4001483

Naj, A. C., Jun, G., Beecham, G. W., Wang, L. S., Vardarajan, B. N., Buros, J., . . . Schellenberg, G. D. (2011). Common variants at MS4A4/MS4A6E, CD2AP, CD33 and EPHA1 are associated with late-onset Alzheimer's disease. *Nat Genet, 43*(5), 436-441. doi: 10.1038/ng.801

Noble, W., Hanger, D. P., Miller, C. C., & Lovestone, S. (2013). The importance of tau phosphorylation for neurodegenerative diseases. *Front Neurol, 4*, 83. doi: 10.3389/fneur.2013.00083

Nordstedt, C., Caporaso, G. L., Thyberg, J., Gandy, S. E., & Greengard, P. (1993). Identification of the Alzheimer beta/A4 amyloid precursor protein in clathrin-coated vesicles purified from PC12 cells. *J Biol Chem, 268*(1), 608-612.

O'Brien, R. J., & Wong, P. C. (2011). Amyloid precursor protein processing and Alzheimer's disease. *Annual review of neuroscience, 34*, 185-204. doi: 10.1146/annurev-neuro-061010-113613

Oh, E. S., Savonenko, A. V., King, J. F., Fangmark Tucker, S. M., Rudow, G. L., Xu, G., . . . Troncoso, J. C. (2009). Amyloid precursor protein increases cortical neuron size in transgenic mice. *Neurobiol Aging, 30*(8), 1238-1244. doi: 10.1016/j.neurobiolaging.2007.12.024

Parikh, I., Fardo, D. W., & Estus, S. (2014). Genetics of PICALM expression and Alzheimer's disease. *PLoS One, 9*(3), e91242. doi: 10.1371/journal.pone.0091242

Parikh, I., Medway, C., Younkin, S., Fardo, D. W., & Estus, S. (2014). An intronic PICALM polymorphism, rs588076, is associated with allelic expression of a PICALM isoform. *Mol Neurodegener, 9*(1), 32. doi: 10.1186/1750-1326-9-32

Paul Flicek, I. A., M. Ridwan Amode, Daniel Barrell, Kathryn Beal, Simon Brent, Denise Carvalho-Silva, Peter Clapham, Guy Coates, Susan Fairley, Stephen Fitzgerald, Laurent Gil, Carlos Garcia-Girón, Leo Gordon, Thibaut Hourlier, Sarah Hunt, Thomas Juettemann, Andreas Kähäri, Stephen Keenan, Monika Komorowska, Eugene Kulesha, Ian Longden, Thomas Maurel, William McLaren, Mattieu Muffato, Rishi Nag, Bert Overduin, Miguel Pignatelli, Bethan Pritchard, Emily Pritchard, Harpreet Singh Riat, Graham R. S. Ritchie, Magali Ruffier, Michael Schuster, Daniel Sheppard, Daniel Sobral, Kieron Taylor, Anja Thormann, Stephen Trevanion, Simon White, Steven P. Wilder, Bronwen L. Aken, Ewan Birney, Fiona Cunningham, Ian Dunham, Jennifer Harrow, Javier Herrero, Tim J. P. Hubbard, Nathan Johnson, Rhoda Kinsella, Anne Parker, Giulietta Spudich, Andy Yates, Amonida Zadissa and Stephen M. J. Searle.). *Ensembl 2013*. [41]. Nucleic Acids Research 2013 41 Database issue:D48-D55.

Pedraza, O., Allen, M., Jennette, K., Carrasquillo, M., Crook, J., Serie, D., . . . Ertekin-Taner, N. (2014). Evaluation of memory endophenotypes for association with CLU, CR1, and PICALM variants in black and white subjects. *Alzheimers Dement, 10*(2), 205-213. doi: 10.1016/j.jalz.2013.01.016

Perl, D. P. (2010). Neuropathology of Alzheimer's disease. *Mt Sinai J Med, 77*(1), 32-42. doi: 10.1002/msj.20157

Pham, M. H., Bonello, G. B., Castiblanco, J., Le, T., Sigala, J., He, W., & Mummidi, S. (2012). The rs1024611 regulatory region polymorphism is associated with CCL2 allelic expression imbalance. *PLoS One, 7*(11), e49498. doi: 10.1371/journal.pone.0049498

Piaceri, I., Bagnoli, S., Lucenteforte, E., Mancuso, M., Tedde, A., Siciliano, G., . . . Nacmias, B. (2011). Implication of a genetic variant at PICALM in Alzheimer's disease patients and centenarians. *J Alzheimers Dis, 24*(3), 409-413. doi: 10.3233/JAD-2011-101791

Purcell, S., Neale, B., Todd-Brown, K., Thomas, L., Ferreira, M. A., Bender, D., . . . Sham, P. C. (2007). PLINK: a tool set for whole-genome association and

population-based linkage analyses. *Am J Hum Genet, 81*(3), 559-575. doi: 10.1086/519795

Ramanan, V., Agrawal, N. J., Liu, J., Engles, S., Toy, R., & Radhakrishnan, R. (2011a). Systems biology and physical biology of clathrin-mediated endocytosis. *Integr Biol (Camb), 3*(8), 803-815. doi: 10.1039/c1ib00036e

Ramanan, V., Agrawal, N. J., Liu, J., Engles, S., Toy, R., & Radhakrishnan, R. (2011b). Systems biology and physical biology of clathrin-mediated endocytosis. *Integrative biology : quantitative biosciences from nano to macro, 3*(8), 803-815. doi: 10.1039/c1ib00036e

Ridge, P. G., Mukherjee, S., Crane, P. K., Kauwe, J. S., & Alzheimer's Disease Genetics, C. (2013). Alzheimer's disease: analyzing the missing heritability. *PLoS One, 8*(11), e79771. doi: 10.1371/journal.pone.0079771

Roch, J. M., Masliah, E., Roch-Levecq, A. C., Sundsmo, M. P., Otero, D. A., Veinbergs, I., & Saitoh, T. (1994). Increase of synaptic density and memory retention by a peptide representing the trophic domain of the amyloid beta/A4 protein precursor. *Proc Natl Acad Sci U S A, 91*(16), 7450-7454.

Rosenbloom KR, S. C., Malladi VS, Dreszer TR, Learned K, Kirkup VM, Wong MC, Maddren M, Fang R, Heitner SG, Lee BT, Barber GP, Harte RA, Diekhans M, Long JC, Wilder SP, Zweig AS, Karolchik D, Kuhn RM, Haussler D, Kent WJ. . (2012). ENCODE Data in the UCSC Genome Browser: year 5 update. *Nucleic Acids Res*.

Sadler, J. E. (1998). Biochemistry and genetics of von Willebrand factor. *Annu Rev Biochem, 67*, 395-424. doi: 10.1146/annurev.biochem.67.1.395

Sagare, A. P., Bell, R. D., & Zlokovic, B. V. (2012). Neurovascular dysfunction and faulty amyloid beta-peptide clearance in Alzheimer disease. *Cold Spring Harb Perspect Med, 2*(10). doi: 10.1101/cshperspect.a011452

Schellenberg, G. D., Bird, T. D., Wijsman, E. M., Orr, H. T., Anderson, L., Nemens, E., . . . et al. (1992). Genetic linkage evidence for a familial Alzheimer's disease locus on chromosome 14. *Science, 258*(5082), 668-671.

Schjeide, B. M., Schnack, C., Lambert, J. C., Lill, C. M., Kirchheiner, J., Tumani, H., . . . Bertram, L. (2011). The role of clusterin, complement receptor 1, and phosphatidylinositol binding clathrin assembly protein in Alzheimer disease risk and cerebrospinal fluid biomarker levels. *Arch Gen Psychiatry, 68*(2), 207-213. doi: 10.1001/archgenpsychiatry.2010.196

Schneider, A., Biernat, J., von Bergen, M., Mandelkow, E., & Mandelkow, E. M. (1999). Phosphorylation that detaches tau protein from microtubules (Ser262, Ser214) also protects it against aggregation into Alzheimer paired helical filaments. *Biochemistry, 38*(12), 3549-3558. doi: 10.1021/bi981874p

Schnetz-Boutaud, N. C., Hoffman, J., Coe, J. E., Murdock, D. G., Pericak-Vance, M. A., & Haines, J. L. (2012). Identification and confirmation of an exonic splicing enhancer variation in exon 5 of the Alzheimer disease associated PICALM gene. *Ann Hum Genet, 76*(6), 448-453. doi: 10.1111/j.1469-1809.2012.00727.x

Scotland, P. B., Heath, J. L., Conway, A. E., Porter, N. B., Armstrong, M. B., Walker, J. A., . . . Wechsler, D. S. (2012). The PICALM protein plays a key role in iron homeostasis and cell proliferation. *PLoS One, 7*(8), e44252. doi: 10.1371/journal.pone.0044252

Selkoe, D. J. (1998). The cell biology of beta-amyloid precursor protein and presenilin in Alzheimer's disease. *Trends Cell Biol, 8*(11), 447-453.

Seshadri, S., Fitzpatrick, A. L., Ikram, M. A., DeStefano, A. L., Gudnason, V., Boada, M., . . . Breteler, M. M. (2010). Genome-wide analysis of genetic loci associated with Alzheimer disease. *JAMA, 303*(18), 1832-1840. doi: 10.1001/jama.2010.574

Shankar, G. M., & Walsh, D. M. (2009). Alzheimer's disease: synaptic dysfunction and Abeta. *Mol Neurodegener, 4*, 48. doi: 10.1186/1750-1326-4-48

Shaw, L. M., Vanderstichele, H., Knapik-Czajka, M., Clark, C. M., Aisen, P. S., Petersen, R. C., . . . Alzheimer's Disease Neuroimaging, I. (2009). Cerebrospinal fluid biomarker signature in Alzheimer's disease neuroimaging initiative subjects. *Ann Neurol, 65*(4), 403-413. doi: 10.1002/ana.21610

Sherrington, R., Rogaev, E. I., Liang, Y., Rogaeva, E. A., Levesque, G., Ikeda, M., . . . St George-Hyslop, P. H. (1995). Cloning of a gene bearing missense mutations in early-onset familial Alzheimer's disease. *Nature, 375*(6534), 754-760. doi: 10.1038/375754a0

Sherry, S. T., Ward, M. H., Kholodov, M., Baker, J., Phan, L., Smigielski, E. M., & Sirotkin, K. (2001). dbSNP: the NCBI database of genetic variation. *Nucleic Acids Res, 29*(1), 308-311.

Silliman, C. C., McGavran, L., Wei, Q., Miller, L. A., Li, S., & Hunger, S. P. (1998). Alternative splicing in wild-type AF10 and CALM cDNAs and in AF10-CALM and CALM-AF10 fusion cDNAs produced by the t(10;11)(p13-14;q14-q21) suggests a potential role for truncated AF10 polypeptides. *Leukemia, 12*(9), 1404-1410.

Smith, R. M., Webb, A., Papp, A. C., Newman, L. C., Handelman, S. K., Suhy, A., . . . Sadee, W. (2013). Whole transcriptome RNA-Seq allelic expression in human brain. *BMC Genomics, 14*, 571. doi: 10.1186/1471-2164-14-571

Steiner, H. (2004). Uncovering gamma-secretase. *Current Alzheimer research, 1*(3), 175-181.

Sweet, R. A., Seltman, H., Emanuel, J. E., Lopez, O. L., Becker, J. T., Bis, J. C., . . . Kuller, L. H. (2012). Effect of Alzheimer's disease risk genes on trajectories of cognitive function in the Cardiovascular Health Study. *Am J Psychiatry, 169*(9), 954-962. doi: 10.1176/appi.ajp.2012.11121815

Tai, H. C., Serrano-Pozo, A., Hashimoto, T., Frosch, M. P., Spires-Jones, T. L., & Hyman, B. T. (2012). The synaptic accumulation of hyperphosphorylated tau oligomers in Alzheimer disease is associated with dysfunction of the ubiquitin-proteasome system. *The American journal of pathology, 181*(4), 1426-1435. doi: 10.1016/j.ajpath.2012.06.033

Tebar, F., Bohlander, S. K., & Sorkin, A. (1999). Clathrin assembly lymphoid myeloid leukemia (CALM) protein: localization in endocytic-coated pits, interactions with clathrin, and the impact of overexpression on clathrin-mediated traffic. *Mol Biol Cell, 10*(8), 2687-2702.

Thomas, R. S., Lelos, M. J., Good, M. A., & Kidd, E. J. (2011). Clathrin-mediated endocytic proteins are upregulated in the cortex of the Tg2576 mouse model of Alzheimer's disease-like amyloid pathology. *Biochem Biophys Res Commun, 415*(4), 656-661. doi: 10.1016/j.bbrc.2011.10.131

Tian, Y., Chang, J. C., Fan, E. Y., Flajolet, M., & Greengard, P. (2013). Adaptor complex AP2/PICALM, through interaction with LC3, targets Alzheimer's APP-CTF for terminal degradation via autophagy. *Proc Natl Acad Sci U S A, 110*(42), 17071-17076. doi: 10.1073/pnas.1315110110

Treusch, S., Hamamichi, S., Goodman, J. L., Matlack, K. E., Chung, C. Y., Baru, V., . . . Lindquist, S. (2011). Functional links between Abeta toxicity, endocytic trafficking, and Alzheimer's disease risk factors in yeast. *Science, 334*(6060), 1241-1245. doi: 10.1126/science.1213210

Wilson, A. C., Dugger, B. N., Dickson, D. W., & Wang, D. S. (2011). TDP-43 in aging and Alzheimer's disease - a review. *Int J Clin Exp Pathol, 4*(2), 147-155.

Wu, F., Matsuoka, Y., Mattson, M. P., & Yao, P. J. (2009). The clathrin assembly protein AP180 regulates the generation of amyloid-beta peptide. *Biochem Biophys Res Commun, 385*(2), 247-250. doi: 10.1016/j.bbrc.2009.05.050

Wu, F., Mattson, M. P., & Yao, P. J. (2010). Neuronal activity and the expression of clathrin-assembly protein AP180. *Biochem Biophys Res Commun, 402*(2), 297-300. doi: 10.1016/j.bbrc.2010.10.018

Xiao, Q., Gil, S. C., Yan, P., Wang, Y., Han, S., Gonzales, E., . . . Lee, J. M. (2012). Role of phosphatidylinositol clathrin assembly lymphoid-myeloid leukemia (PICALM) in intracellular amyloid precursor protein (APP) processing and amyloid plaque pathogenesis. *J Biol Chem, 287*(25), 21279-21289. doi: 10.1074/jbc.M111.338376

Xu, W., Tan, L., & Yu, J. T. (2014). The Role of PICALM in Alzheimer's Disease. *Mol Neurobiol*. doi: 10.1007/s12035-014-8878-3

Xu, X., Wang, H., Zhu, M., Sun, Y., Tao, Y., He, Q., . . . Saffen, D. (2011). Next-generation DNA sequencing-based assay for measuring allelic expression imbalance (AEI) of candidate neuropsychiatric disorder genes in human brain. *BMC Genomics, 12*, 518. doi: 10.1186/1471-2164-12-518

Young-Pearse, T. L., Bai, J., Chang, R., Zheng, J. B., LoTurco, J. J., & Selkoe, D. J. (2007). A critical function for beta-amyloid precursor protein in neuronal migration revealed by in utero RNA interference. *J Neurosci, 27*(52), 14459-14469. doi: 10.1523/JNEUROSCI.4701-07.2007

Yu, J. T., Song, J. H., Ma, T., Zhang, W., Yu, N. N., Xuan, S. Y., & Tan, L. (2011). Genetic association of PICALM polymorphisms with Alzheimer's disease in Han Chinese. *Journal of the neurological sciences, 300*(1-2), 78-80. doi: 10.1016/j.jns.2010.09.027

Vita
Ishita Jatin Parikh

Education

Austin Peay State University, **Clarksviile, TN** **2003-2007**
B.S. in Biology, Cum Laude
Minor in Chemistry, Mathematics and Leadership

Research & Professional Experience

Graduate Student, University of Kentucky 2009-2014
Mentor: Steven Estus, Ph.D.

Research Assistant, Vanderbilt University 2009
Mentor: Lisa McCawley, Ph.D

Undergraduate Researcher, Austin Peay State University 2005-2007
Mentor: Gilbert Pitts, Ph.D.

Teaching Experience

University of Kentucky, Lexington, KY Fall 2012
Teaching Assistant, PGY 207

Students Mentored

Mark Vinas, Undergraduate student 2014
Carson Van Sanford, Medical student 2012

Professional Memberships

Society for Neuroscience 2011-2014

Publications

Parikh I, Medway C, Younkin S, Fardo DW, Estus S. An intronic PICALM polymorphism, rs588076, is associated with allelic expression of a PICALM isoform. Molecular Neurodegeneration. 2014;9(1):32. PMID: 25169757.

Nelson PT, Estus S, Abner EL, **Parikh I**, Malik M, *et al*. ABCC9 gene polymorphism is associated with hippocampal sclerosis of aging pathology. Acta neuropathologica. 2014;127(6):825-43. PubMed PMID: 24770881.

Parikh I, Fardo DW, Estus S. Genetics of PICALM expression and Alzheimer's disease. PloS one. 2014;9(3):e91242. PubMed PMID: 24618820.

Malik M, Simpson JF, **Parikh I**, Wilfred BR, Fardo DW, Nelson PT, Estus S. CD33 Alzheimer's Risk-Altering Polymorphism, CD33 Expression, and Exon 2 Splicing. The Journal of Neuroscience : 2013;33(33):13320-5. PubMed PMID: 23946390.

Abstracts

I. Parikh, J. Simpson and S. Estus. *Genetics of PICALM gene expression and Alzheimer's Disease.* ApoE, ApoE Receptors and Neurodegeneration, Lexington, KY **2014**.

I. Parikh, J. Simpson and S. Estus. *Alzheimer's associated gene PICALM: expression and splicing in the human brain.* Society for Neuroscience, San Diego, CA **2013**.

I. Parikh, J. Simpson and S. Estus. *Molecular characterization of splicing of the Alzheimer's-associated gene PICALM in the human brain*. ApoE, ApoE Receptors and Neurodegeneration, Washington, D.C. **2013**.

I. Parikh, J. Simpson and S. Estus. *PICALM SNP Associated with Alzheimer's Disease: Expression and Splicing.* International Conference on Alzheimer's and Parkinson's Diseases, Florence, Italy **2013**.

I. Parikh, J. Simpson and S. Estus. *Do Alzheimer's Disease associated SNPs alter expression or splicing of PICALM?* Society for Neuroscience , New Orleans, LA **2012**.

I. Parikh and S. Estus. *Molecular characterization of expression of the Alzheimer's-associated gene PICALM in the human brain*. ApoE, ApoE Receptors and Neurodegeneration, Jacksonville, FL **2012**.

I. Parikh and S. Estus. *Molecular characterization of expression of the Alzheimer's-associated gene PICALM in the human brain*. Markesbery Symposium on Aging and Dementia, Lexington, KY **2011**. *Outstanding Poster Award*

I. Parikh and S. Estus. *Molecular characterization of expression of the Alzheimer's-associated gene PICALM in the human brain*. Society for Neuroscience ,Washington, D.C. **2011**.

I. Parikh and S. Estus. *Molecular characterization of expression of the Alzheimer's-associated gene PICALM in the human brain*. ApoE, ApoE Receptors and Neurodegeneration, Chicago, IL **2011**.